

## Final Scientific/Technical Report

### Item #1:

SBIR Grant #DE-FG02-04ER83902, Applied Physics and Measurements, Inc.

“Using Downhole Probes to Locate and Characterize Buried Transuranic and Mixed Low Level Waste.”

Principal Investigator: Donald K. Steinman.

Item #2, Also On Cover Sheet: Distribution Limitations.

### Item #3, Executive Summary:

The research presented in this report has advanced the technology needed to quantify high and low concentrations of chlorinated hydrocarbon waste materials often found with Transuranic (TRU) and mixed low level waste (MLLW) in US DOE Weapons Complex sites around the country. This was accomplished by applying borehole logging technology developed in the oil and gas exploration and production industry and borehole logging technology from uranium exploration. Three instruments were used in this work. These technologies were modified to optimize their effectiveness for solving problems in TRU and MLLW quantification in burial pits and leakage plumes. Based on logging tools originally developed for the INEEL in 2000 through 2003, this project refined the instruments and used them to demonstrate sensitivity to TRU and volatile organic compounds (VOC) over a wide range of concentrations. One instrument uses a uranium exploration technique, prompt fission neutron (PFN) logging, to measure plutonium concentrations as low as 1.5 nCi/gm. The second uses pulsed neutron-capture (PNC) to measure chlorine concentration in soils fully saturated with carbon tetrachloride. The third, the prompt neutron-gamma (PNG) uses a pulsed neutron generator with a high purity germanium diode detector to measure as little as twenty-five parts per million (ppm) chlorine in soils.

The logging methods were developed at a laboratory site in Houston, TX that has a subsurface installation for simulating the soils of the repositories. Several over-pack drums were filled with mixtures of materials to simulate the subsurface environment encountered at the Weapons Complex storage sites, and the response of the tools to the materials in the drums was measured. These surrogate drums represented a variety of subsurface conditions as well as some conditions needed to accurately characterize the responses of the tools to certain elementary conditions. For example, one drum was filled with diesel fuel in order to measure the response of the PNG to carbon. Most surrogates are closely related to the vadose soil conditions encountered in the Rocky Mountain West areas similar to INL and Hanford.

This is a cost effective method of developing the response of these tools. The method is used extensively in the oilfield services industry to prepare response charts for interpretation of the downhole logs the tools are designed to make. Using these surrogates we prepared response diagrams and formulas to interpret the signals from the PNG and PNC tools. The PFN could only be calibrated using the uranium calibration models at the Hanford site.

Prior to the present work, the Weapons Complex sites used a variety of methods to quantify the VOC and TRU content of the subsurface. Physical sampling is both expensive and hazardous because of the potential for releasing the materials into the surface. Prior logging techniques have not had the sensitivity or specificity to measure these materials at important concentration levels. The methods developed here make it possible to survey such sites as Hanford and INL for TRU and VOC's significantly less expensively than by using drilling and sampling. In addition, in many of these waste depositories the distribution of materials is highly heterogeneous. Sampling usually involves obtaining

only cubic centimeter sized volumes. The tools developed here measure volumes of material of approximately two cubic feet, thus producing a more representative measurement.

These tools represent a cost effective approach to learning the contents of the subsurface in the Weapons Complex waste fields. The measurement capability was demonstrated at Hanford during summer 2008, and the report of that activity is appended to this report. (Appendix 2).

Item #4: Actual Accomplishments Compared to Goals and Objectives of Project:

As stated in the APMI proposal for this Grant, there were three technical objectives:

- Modify the PFN and PNG logging tools based on lessons learned during the development project in which the tools were constructed and initially tested. (These were the tools built originally at INEEL and supplied to this project on a no-cost basis from the INL.)
- Characterize the responses of the tools using test fixtures, the calibrated uranium pits at Grand Junction, and further MCNP modeling and develop interpretation methods.
- Conduct logging operations in the SDA at the ICP, and analyze the data acquired during the operations.

**The first objective** was straightforward to accomplish. The tools were modified during the early months of the project by removing the cumbersome downhole power supplies. This permitted the PFN to achieve full output and the PNG to be easier to fill with liquid nitrogen and to be assembled at a well site. We also modified the germanium detector by replacing the digital front end preamplifier with a standard preamplifier. This resulted in no more detector failures compared to two previous failures with the digital device. A common cable head was constructed that permitted both tools to be run on the cable with minimal assembly time when using the tools downhole. The Zetatron-based PFN was extremely reliable during this project. The other generator, the A-320 was significantly less so because it had been a one-of-a-kind from the vendor. However, we were able to coax out of it sufficient use to demonstrate those measurement features that were intended to be shown.

One feature of the tools from INL that had never been tested was the substitution of NaI gamma ray detectors for the  $^3\text{He}$  PFN detectors. APMI added the NaI detectors and used them to make PNC measurements in both the Houston test facilities and at Hanford during the demonstration there. They proved to be an invaluable addition to this technology development by enabling us to measure extreme chlorine concentrations accurately.

We believe, therefore:

This objective was met fully during the project.

**The second objective** was also straightforward, and most aspects were accomplished. Among the equipment provided from INL were five surrogate drums (83-gallon overpacks) that had been built in Idaho to resemble the soil at the RWMC. APMI fabricated an additional four drums in overpacks to simulate the effects of small amounts of chlorine on the tool responses. In addition, we fabricated a drum filled with diesel and salt to simulate extreme chlorine concentrations and very high carbon environments.

We also refined the MCNP simulations of tool responses in order to interpret experimental results we were getting from the tool measurements in the surrogate drums. We were able to benchmark the MCNP results to results obtained from the surrogate formations. From those results, we developed data interpretation methods to enable us to extract information from field logs.

There were three principle thrusts in data analysis. The first was to use Genie, a Canberra product that was used to analyze the spectral data from the high-purity Ge detector. The second was a dual exponential fitting code to analyze the time decay modes of the PNC tool. The third was an Excel spreadsheet template that analyzed the time decay data from both the PNC and the PFN tools to provide quick and accurate analysis during and immediately after data acquisition. Using these tools we were able to analyze the data from all three tools and use the results in our work at the Hanford site.

Because of time and budget constraints, we were unable to use the characterization facilities at Grand Junction, CO. However, the calibration models at Hanford were produced in the same manner as those in Grand Junction, and we calibrated the PFN and the passive response of the PNG tool in those formations.

We believe, therefore:

This objective was met fully during the project.

**The third objective**, logging at the SDA at ICP was altered. During the course of the project there were modifications to this objective because of modifications of the work scope at the Idaho Clean-up Project (ICP). Early in the project, our contacts at ICP and INL suggested that measuring chlorine concentrations in the vadose zone that were saturated with carbon tetrachloride would be valuable to ICP. We then added high chlorine measurements to our project plan. However, during the course of our work ICP decided that they needed no further characterization of the SDA at RWMC, and they declined to participate in the field demonstration. We decided to find other locations that would benefit from the technology, and Hanford proved a willing partner in this operation. We conducted field operations at Hanford during the summer of 2008, and the results from that work are appended to this report.

We believe, therefore:

This objective was met fully during the project.

#### Item #5: Summary of project activities

The project goal was to develop technology to identify and quantify a wide range of concentrations of TRU and VOC waste in subsurface disposal and storage areas of the DOE Weapons Complex sites and to demonstrate that technology at one of the Weapons Complex sites.

During the project we developed pulsed neutron borehole logging tools perform the required measurements. Three tools were tested during this project:

1. A Prompt Fission Neutron (PFN) tool to measure fissionable material,
2. A Pulsed Neutron Capture (PNC) tool with which we measure chlorine at very high concentrations, and
3. A Pulsed Neutron Gamma (PNG) tool for measuring chlorine and other elemental concentrations from the parts-per-million range to the few percent concentration range

Analysis of data taken at the APMI laboratory in Houston, TX and at the calibration facilities at Hanford shows that these instruments can measure:

- Plutonium at the level of ~1 nCi/gm in a three minute count,
- Chlorine accurately in soil saturated with CCl<sub>4</sub> using the PNC tool with a 3 minute measurement, and

- Chlorine accurately at 16 parts per million using the PNG tool.

During July 2008 APMI demonstrated the logging tools at the Hanford site with additional funding provided by the Department of Energy through Fluor Hanford. APMI was introduced to Fluor Hanford with help from Foresight Science and Technology whose personnel developed a commercialization plan for us.

Since the inception of the project as a Phase I Grant, the following work has been accomplished:

**During Phase I** a Monte Carlo model (using MCNP) of the PFN logging tool was developed and benchmarked against data acquired at INL. The experiments at INL consisted of logging the tool past a NAD plutonium source placed in a surrogate formation at different radial distances from the borehole. There was no way to correlate the exact amplitude of the response because the tool's downhole power supply and control system did not permit the neutron generator to achieve its full output. The shape of the response as a function of the vertical and radial position of the source was accurately modeled.

A MCNP model of the PNG was also developed and used to assess the sensitivity to chlorine and carbon.

The original technical goal was to develop a capability in the tools to locate both the vertical and radial disposition of materials behind the casing by using the differences in the response of the near and far detectors of the PFN and the differential attenuation of gamma rays from select materials using the PNG tool. Phase I activities demonstrated this capability; however, the needs of the perceived end-users were in assessing both low level and high level chlorine concentration. Thus during Phase II, emphasis shifted to establishing that capability.

**Upon commencement of Phase II**, we began to build the laboratory site at NSSI in Houston. INL agreed to lend the equipment from the original development project to APMI for the purposes of the SBIR Grant. When the lending agreement was in place, we sent the two neutron generators to the vendor, Thermo-Fisher Corp. in Colorado Springs, CO. They determined that the tubes were no longer functional because they had not been exercised in the last year and a half. At additional and unanticipated cost to the project, they were replaced. We made a trip to CO to get the A320 generator functional with the help of Thermo-Fisher personnel. Thereafter, APMI exercised the generators at least every 6 weeks to ensure they were always operational. Somewhat later into the program, it was determined that the tube in the A320 had ceased to work, and it was replaced under warranty by Thermo-Fisher. However, throughout the project, operation of the A320 was problematical. The generator had been built as a special unit for INL, and there was only one of its kind. It suffered frequently from component and wiring failures. APMI made a decision to limit repair efforts on the A320 to keeping it minimally functional because a full reworking of the system would have depleted project resources. Even so, it took several man-months of effort and several thousand dollars of project funds to get the generator to a state where we could collect useful data.

To address the need for a measurement of high chlorine concentrations, it was decided to utilize the PNC technique familiar in the oilfield to quantify brine behind casing. This required that we add the NaI gamma ray detector package to the Zetatron system in the PFN tool. This was accomplished directly with only minor equipment modifications.

By spring of 2006, the lab was operational, and we began making measurements. The first measurements employed the PNC tool to measure the neutron capture cross section,  $\Sigma_a$ , in the drums from INL. We also began a series of MCNP simulations in order to understand the results we were obtaining.

We also began the effort to render the PNG operational in Q3, 2006. This became a major activity for several months. It was determined after a few weeks of work that the neutron generator tube had failed. It was replaced by Thermo-Fisher under warranty. We then assembled the neutron generator and the high purity Ge detector. Upon running the tool we discovered that the electronic noise from the generator broadened the resolution of the detector excessively. Several more weeks were required to reduce the resolution to a useable figure ( $< 3$  keV FWHM). In early 2007, we began making measurements with the PNG on the INL surrogates, and we built four additional surrogates to ensure we understood the response in both low chlorine environments and high chlorine environments. One surrogate consisted of salt (NaCl) pellets and diesel oil. This allowed us to examine high chlorine and high carbon concentrations in one data run.

After logging the eight tanks using both the PNG and the PNC tools, we focused on analyzing data from the runs. We were able to demonstrate with the data from the tools and from MCNP that we could assess chlorine concentrations ranging from approximately 16 ppm Cl to the concentration of soil fully saturated with  $\text{CCl}_4$ .

The following data and analysis will demonstrate the results of the experimental and computational program.

1. PNC cross section logging and analysis
2. PNG chlorine logging and analysis
3. PFN logs at Hanford
  - a. Calibration
  - b. Well logs
  - c. MCNP analysis

The first four points are described in Appendix 1; the Hanford work is described in Appendix 2.

After performing the tool characterization studies at NSSI, APMI conducted a two week operation at the Hanford site to demonstrate the measurement capabilities of the logging tools. We ran the tools in the following holes:

- Calibration wells SBL/SBH to measure the response of the PFN to uranium. This result was converted to response for Pu.
- Calibration wells SBA/SBB for the PNG without the neutron generator to calibrate the response to Pu in the germanium detector
- Well 73 which had been reported to contain up to 29 nCi/gm of Pu by S. M. Stoller logs. The PFN measured similar amounts.
- Well 69 which had been reported to contain up to 70 nCi/gm of Pu. The PFN measured similar amounts.
- Well 82 in which it was suspected that high levels of chlorine were present. Both the PNC and the PNG showed little or no chlorine in this well.

Data from the demonstration were analyzed, and a set of well logs was delivered to both the DOE and Fluor Hanford. The details of the analysis of the Hanford logs is attached as Appendix 2 to this report.

Item #6: Products developed under award.

As stated above, this project developed three logging tool prototypes for assessing TRU and MLLW in subsurface disposal areas and other subsurface areas containing those materials at DOE Weapons Complex sites. In addition, we developed prototype methods and procedures for analyzing the data from the tools. These systems are ready for deployment in these areas. If the DOE were to embark on further analysis of its subsurface areas, these instruments would be a valuable means to maximize information while minimizing the cost of acquiring the data.

One publication has resulted from Phase I of the grant: Steinman, D. K. and Schweitzer, J. S., "MCNP Modeling Results for Location of Buried TRU Waste Drums," European Physical Society, 19<sup>th</sup> Nuclear Physics Divisional Conference, Pavia, Italy September 5-9, 2005. Paper #441.

### **Item #7: Computer Modeling:**

The responses of the nuclear tools were modeled using MCNP<sup>1</sup> version 1.5.1. A separate model was developed for each tool configuration, and separate models were constructed for the surrogate formations and for formations of infinite extent. In each case a 14 MeV neutron source was used and the geometry and materials known to be around the generator tube was constructed. The detector locations and sizes were taken directly from tool dimensions. Materials in each of the surrogate formations were known relatively precisely because of how they were constructed. Materials in earth formations were chosen based on data supplied by personnel at Hanford and INL. Several bespoke FORTRAN codes were developed to build input decks for MCNP and to harvest the tallies.

More than 600 cases were computed during the project to evaluate the responses and to understand the behavior of the responses in the various environments used.

The figures below show the PFN model. They are taken from the VisEd program used to build MCNP inputs. The color selection in these figures is limited by the program itself. Even so, the source (the white and green area on top) and the two detectors (in various shades of blue below) are clearly an aid in visualizing the configuration. The PNC tool is very much the same except there are two NaI detectors in the place of the <sup>3</sup>He detectors in the PFN.

The cross sectional view in figure 2 is at the level of the near detectors. The inner array of dark blue circles shows the far epithermal <sup>3</sup>He detectors. The light ring is cadmium to exclude thermal neutrons from the epithermal detector pack. The lighter blue in which the detectors are embedded is polyethylene used to moderate fast and epithermal neutrons coming into the detector pack. It enhances the sensitivity to epithermal neutrons; however, it also slows down the response of the system so that it's difficult to measure epithermal neutrons in a highly absorbing medium. The outer array of four dark blue circles shows the monitor neutron detector. This signal is used to normalize the response of the epithermal detector pack.

---

<sup>1</sup> MCNP-A General Monte Carlo N-Particle Transport Code Version 5," Los Alamos National Laboratory Vols. I-III, April, 2003; and is available from Radiation Safety Information Computational Center at Oak Ridge National Laboratory as CCC-740

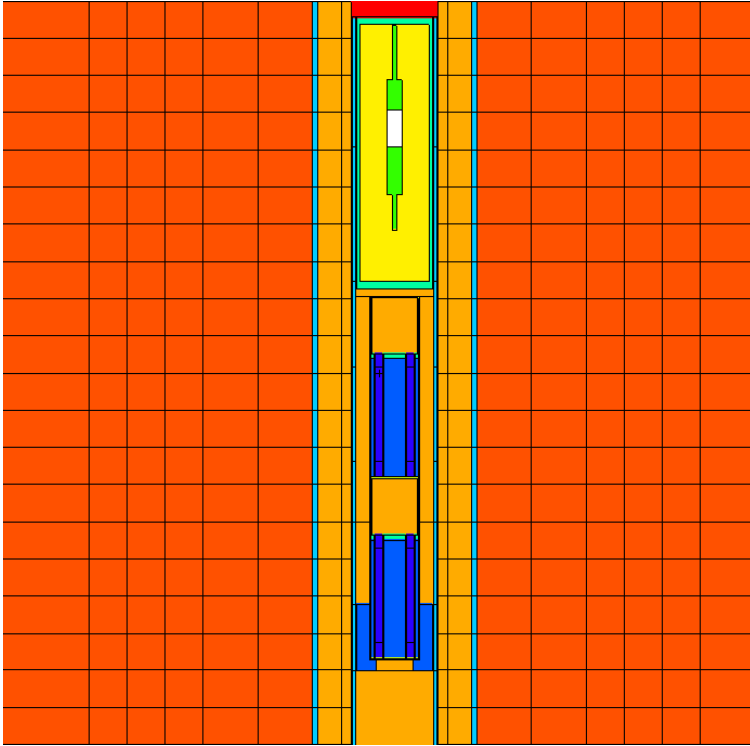


Figure 1 – Longitudinal view of PFN model of the Hanford wells. Deep orange on the outside is the formation; light orange is air surrounding the inside of the tool and the air-filled borehole.

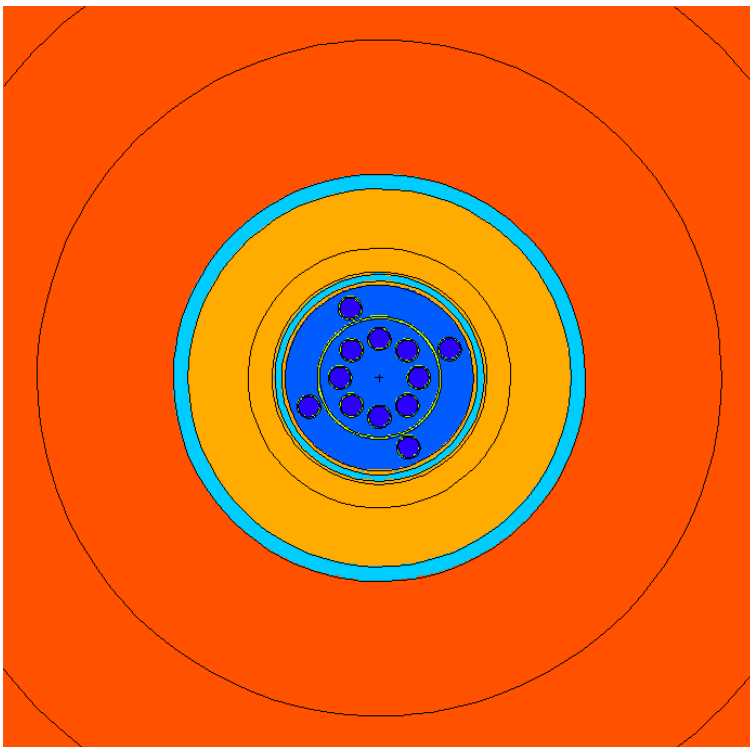


Figure 2 – Cross sectional view of the PFN detector section. The inner ring of 8 detectors are for measuring epithermal neutrons; the outer ring of 4 detectors are monitor neutrons to normalize the epithermal signal.

The output from the PFN and PNC model is a set of time bins with the counts per source neutron. An example is shown in Appendix 3. With the PNC tool decay curves derived from the model results are then used to fit for  $\Sigma_c$ . (see Appendix 1.) Often it is required to fit to a two-exponential curve because the neutron population in the borehole has a different decay time than does that in the formation. With the PFN tool, the counts are simply summed over all times after approximately 400  $\mu$ seconds. It takes that long for the burst neutrons to decay in the polyethylene moderator inside the cadmium shield. It is critical for all the burst neutrons to decay prior to measuring epithermal neutrons. That way one only counts neutrons from fission as a unique signature of fissile material in the environment.

Foresight Science and Technology have helped APMI with technology transfer. They also prepared a market assessment plan for us.



## Appendix 1: Technical Accomplishments

In this appendix we present the data and analysis for the measurement capabilities developed during this grant. In order, they are:

1. PNC cross section logging and analysis
2. PNG chlorine logging and analysis

### PNC Cross Section Logging

Several attempts have been made to use neutron instruments to assess the chlorine content of subsurface spills of volatile organic chemicals (VOC). All work very well at concentrations below 5% Cl by weight, however, above that concentration, the neutron absorption characteristics of Cl cause large errors in the measurement. APMI employed a technique from the oilfield services industry to overcome these problems. The method is thermal decay time, and it is used by many companies to measure the water saturation of hydrocarbon bearing formations behind cemented steel casing. In that case, the range of salinities is from a few ppm to 260,000 ppm. The latter is fully saturated NaCl in water in the pore space in rocks. However, in the Weapons Complex, there are many cases in which carbon tetrachloride was spilled or otherwise accumulated in the rock pore spaces, and that is a significantly larger Cl content.

This tool uses the PFN probe with the NaI detectors instead of the  $^3\text{He}$  detectors. The purpose of the measurements is to determine the macroscopic neutron capture cross section of the formation. This measured quantity is directly related to the chlorine concentration when the chlorine concentration is high. The capture cross section,  $\Sigma_c$ , is determined as shown below:

$$\Sigma_c = \sum_i N_i \sigma_i \quad \text{Eq. (A1)}$$

Where,  $N_i$  is the concentration of atoms of type,  $i$ , in atoms per cubic centimeter, and  $\sigma_i$  is the microscopic capture cross section of atoms of type,  $i$ . Chlorine has a very large cross section compared to the other elements found in the formations of interest, so that when the chlorine concentrations is greater than approximately 1% by weight, chlorine is the dominant term in equation (1) and subsequently dominates the measured cross section  $\Sigma_c$ . For concentrations expected to be seen in the SDA (generally assumed to be in the range of 10 – 25%), chlorine is the only significant term in the equation.

The measurement is performed by inserting a burst of fast neutrons into the formation and measuring the gamma rays resulting from capture of the burst neutrons by elements in the formation and other parts of the environment (mainly casing and cement). The neutron burst is slowed to thermal neutron energies (0.025 eV), and the thermal neutron cloud decays exponentially in time according to the equation:

$$N(t) = N_0 * e^{-t/\tau} \quad \text{Eq. (A2)}$$

Where  $\tau$  is the thermal decay time and it is related to  $\Sigma$  by:

$$\tau = 4550/\Sigma_c \quad \text{Eq. (A3)}$$

As stated above, tool detects gamma rays and sorts them into time bins with a time base keyed to the pulse that starts the neutron burst. After detection, the decay time is fitted using standard mathematical

techniques.<sup>2</sup> The decay times are inverted as in Eq. A3, and the sigma values are put out to the log. Figure 3 shows a sigma log in the surrogate formations. Sigma values are computed from both the near and the far NaI detectors. The far detector almost always is the more accurate of the two because it is further from the source, and it has a smaller diffusion component<sup>3</sup>. A further correction was derived using the MCNP results

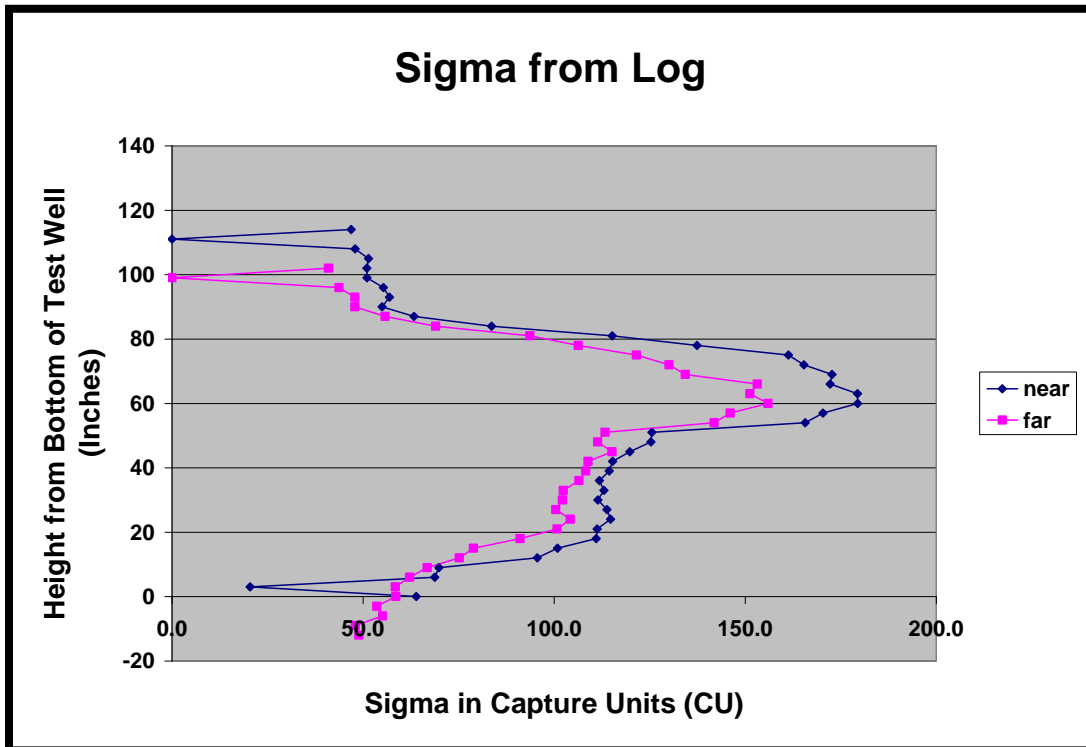
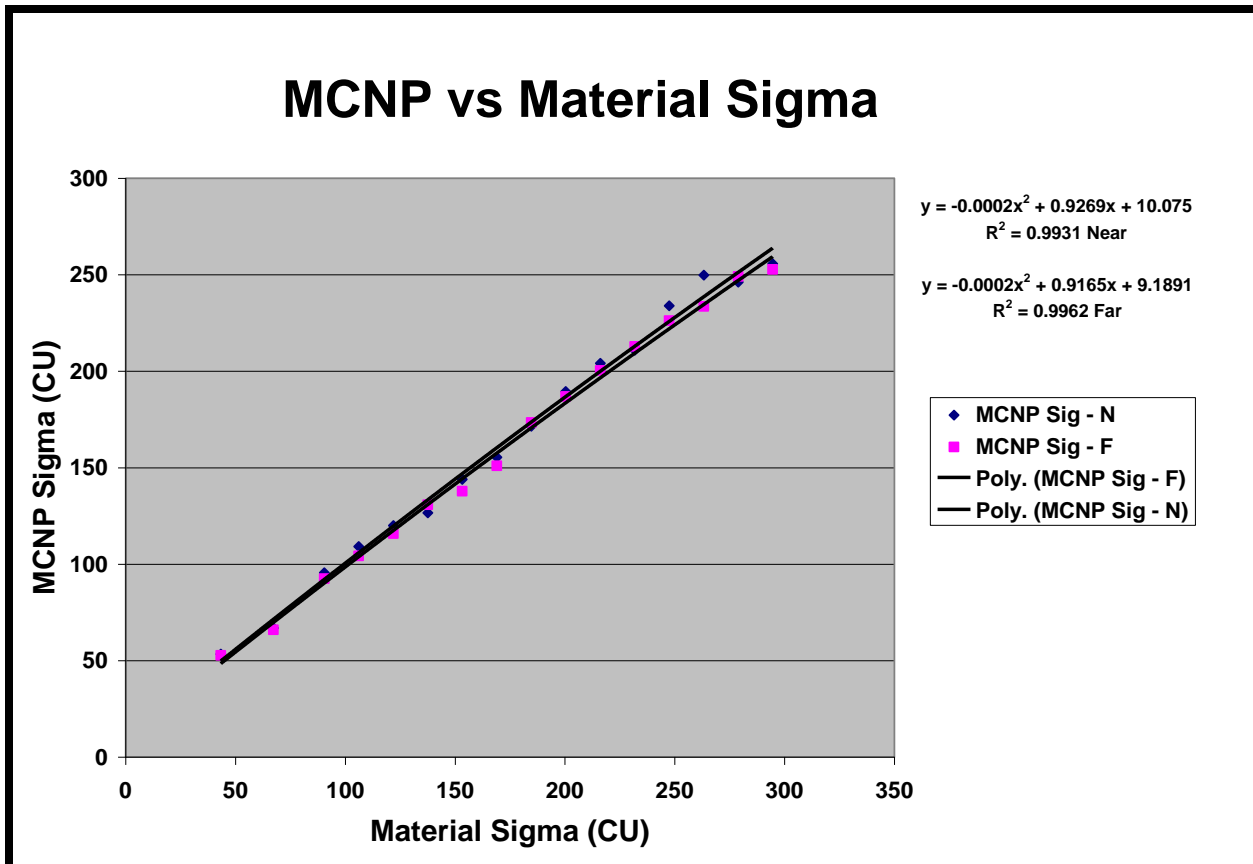


Figure 3 Scan of test well PFN in NaI configuration. Note that spatial resolution of the near detector is sharper than the far detector. The low points at the top and bottom of the log are data drop outs.

The results show that the tool is reading lower values of sigma than expected. The MCNP studies show that the tool is capable of measuring chlorine concentrations above 25% by volume. This corresponds to carbon tetrachloride, the suspected contaminant of the SDA, completely filling the interstitial spaces in the SDA fill soil. Figure 4 shows the results of the MCNP simulation:

<sup>2</sup> Steinman, D.K., Adolph, R.A., Mahdavi, M., and Preeg, W.E., "Dual-Burst Thermal Decay Time Logging Principles," SPE Formation Evaluation, Vol 3, (1988) pp 377 - 385.

<sup>3</sup> The diffusion component arises because the neutron cloud spreads out by neutron diffusion as it gets absorbed. The spreading makes it look to a detector that the cloud is decaying faster than by capture alone. See also footnote #2.



**Figure 4 – Plot of the predicted capture cross section from MCNP vs. sigma computed from the material properties. The equations at the upper right were computed using Excel, and represent the fit of the data to a quadratic. The fact that the quadratic term is small shows that the fit is nearly linear. Thus, MCNP predicts that the PFN in PNC mode is capable of determining very high concentrations of chlorine in the SDA.**

An ad hoc method was developed to correct the measured sigma to the true sigma. This was obtained by making a heuristic fit of the measured data to the results of fitting the dual exponential process of the measured data. First the decay curves were processed to produce a fast (borehole) and slow (formation) decay rates together with the amplitude of the fast and slow signals. It turned out that the amplitude ratios clearly indicate whether the formation is fast or slow. When the formation decay is fast, the ratio is low and vice versa. Given such an indicator, it is straightforward to develop the formula at the top of figure 5.

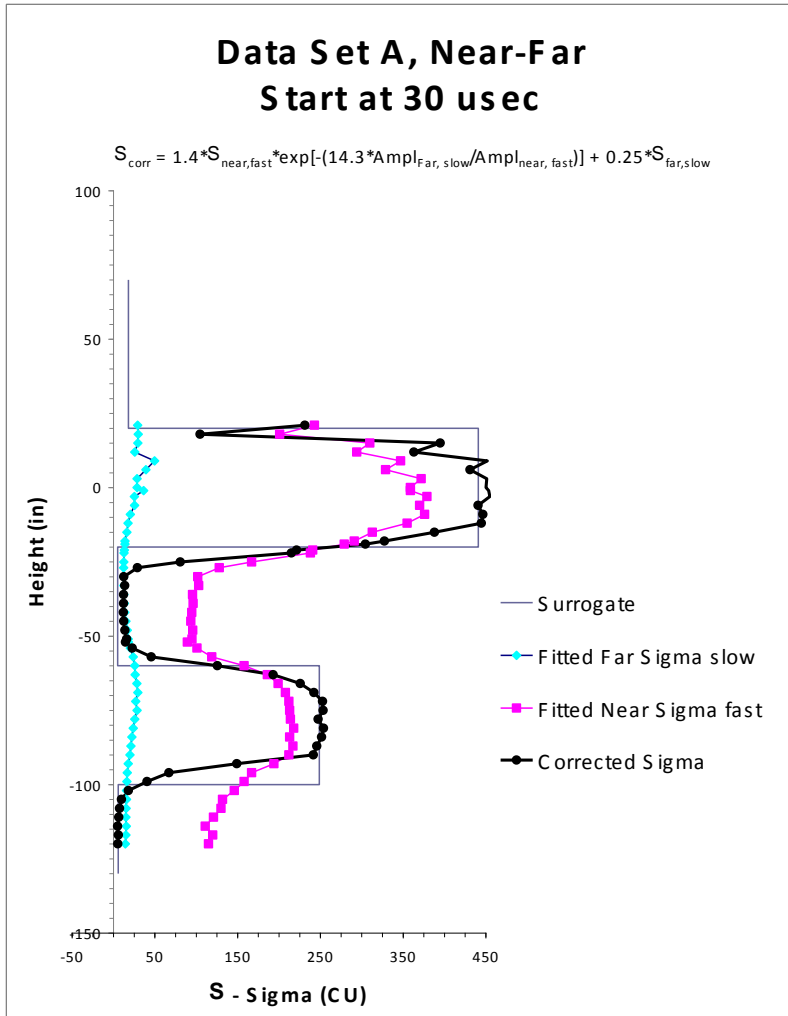


**Figure 5 – Chart showing results of the heuristic fit of the measured data (Near and Far Sigma) to the known true sigma values. The correction is included at the top of the chart. Data were acquired in three contiguous surrogate drums.**

### PNG Chlorine Logs:

It is possible to determine the amount of chlorine in a formation by measuring the capture chlorine peaks in a gamma ray spectrometer. The PNG tool has a germanium diode spectrometer that is used in both active (neutrons on) and passive (neutrons off) modes. In passive mode, the spectrometer is used to measure natural activity (potassium, uranium, and thorium) as well as any active fission product materials (americium, cesium, etc.) in the subsurface. In active mode the tool can measure inelastic gamma rays during the time the neutron burst is active (e.g.; oxygen and carbon), and it measure capture gamma rays between bursts while the neutron cloud from the burst is decaying in the environment near the tool.

Figure 5 shows the response to chlorine in the environment at varying concentrations. At only a few percent concentration, the response decreases as concentration increases because of absorption of the neutrons by chlorine. This absorption will also distort the measurement of other species. However, it is

possible to correct for the absorption by using the value of  $\Sigma_c$  obtained from the PNC tool. Once this is done, the response becomes an increasing function of the concentration as shown in figure 6.

At low concentrations, a tau correction is unneeded. Chlorine can be computed from the net peak area. During the work at Hanford and in Houston, we calibrated the response to low values of chlorine. In a low-absorbing formation (i.e.; where there are no other strongly absorbing species) the tool measures chlorine at the level of less than 25 ppm through the steel casing.

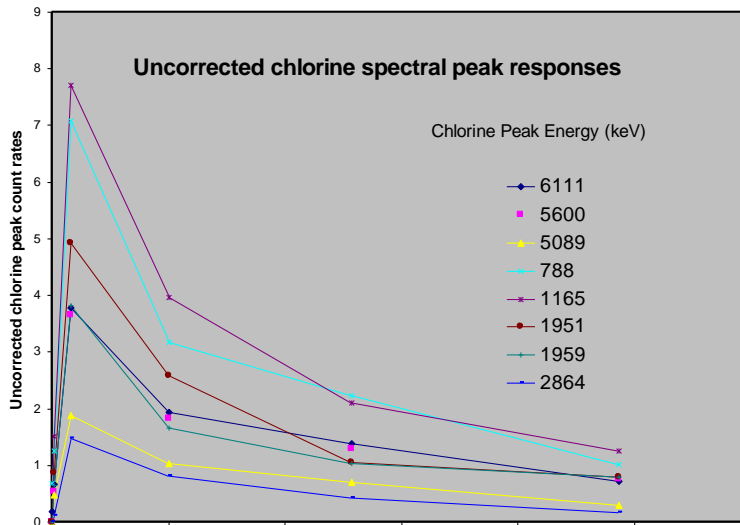


Figure 6 – Gamma ray spectrometer response in the various chlorine capture gamma ray lines as a function of chlorine concentration. Without a correction factor, the count rate actually declines with increasing concentration.

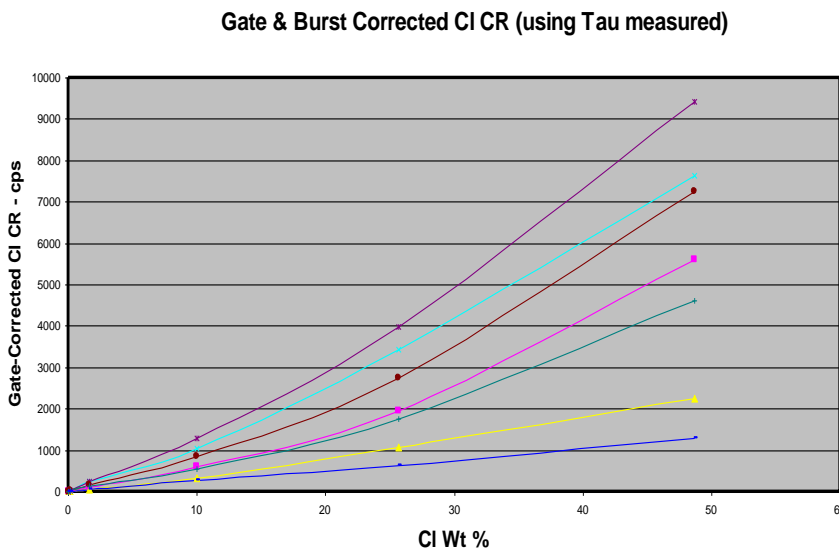


Figure 7 – Corrected response of the PNG to chlorine using the tau value from the PNC tool. With this correction the PNC and PNG chlorine concentrations can be checked for consistency.

Examples of both logs as well as the PFN logs from two wells are described in more detail in Appendix 2.

## **Appendix 2 –Report to Hanford on the Logging Program.**

### **ABSTRACT**

This report contains the results of the work performed by Applied Physics and Measurements, Inc. for Fluor Hanford to demonstrate technology developed during APMI's SBIR Grant that will help solve their monitoring and subsurface characterization program by measuring fissile material and volatile organic compounds in the subsurface.

APMI logged with three (3) tools in three active wells (W10-69, W10-73, and W15-82) at the Hanford site. The tools used are the Prompt Fission Neutron (PFN) for Pu determination, the Pulsed Neutron Capture (PNC) for measuring the formation capture cross section and hence the concentration of Cl in high concentration areas. Finally, the Pulsed Neutron Gamma (PNG) was used to determine Cl at low concentrations and to determine other elements of interest.

These activities produced the following assay results:

1. Plutonium was observed in Wells W10-69 and W10-73 with the PNG (in passive mode) and the concentrations were verified with PFN. The maximum observed concentration in W10-73 was less than previously reported.
2. The sensitivity to plutonium is approximately 1.5 nCi/gm based on a 300 second measurement.
3. Cesium and thallium concentrations in both wells were consistent with previous reports. Other radio nuclides were measured.
4. Evidence for chlorine was found in well W15-82. Analysis of PNG capture spectra indicates the presence of chlorine at the 2,700 parts per million-concentration level. There was no evidence of man-made radio nuclides observed in the zones logged (approximately 40-75 feet) in this well.

Data from this work are sound, although operating the tools was difficult because they are experimental prototypes. Commercial versions of the tools would be smaller, faster in operation, and reliable.

The logs shown in the report are the main results from the test. Other results are shown in an appendix. Additionally, logs measured by S. M. Stoller Corporation are also shown in an appendix as a convenience to the reader.

# Demonstration of Nuclear Probes to Fluor Hanford

*D. K. Steinman (PI), R. L. Bramblett, and R. C. Hertzog, Applied Physics and Measurements, Inc., Missouri City, TX 77459*

## Introduction – Purpose of APMI Hanford Field Trip

This report is the result of Applied Physics and Measurements, Inc. (APMI) work at Fluor Hanford to demonstrate the technology developed during the SBIR Grant to APMI (#DE-FG02-04ER83902 titled “Using Downhole Probes to Locate and Characterize buried Transuranic and Mixed Low Level Waste”) The purpose of this work is to provide Fluor Hanford the evidence that these downhole probes can help their monitoring and subsurface characterization program. APMI met with Hanford personnel in November 2007, and APMI developed a project plan for the demonstration of three logging tools and presentation to Hanford (and DOE) of the results from the demonstration. The accomplishments are described below.

APMI logged three (3) tools in three monitor wells at the Hanford site. The wells were chosen by Fluor Hanford personnel. The tools used are the Prompt Fission Neutron tool (PFN) for plutonium determination, the pulsed neutron capture (PNC) tool for measuring the formation capture cross section and hence the concentration of Cl in high concentration areas. Finally, the pulsed neutron-gamma tool (PNG) is used to determine Cl at low concentrations and to determine other elements of interest. Both passive and active runs were made. The passive runs of the PFN are used to identify or verify areas where Pu and Am are located using the neutrons from spontaneous fission (Pu) and ( $\alpha$ ,n) reactions from the decay of Am and Pu. Passive gamma ray runs can be used to identify or verify Pu isotopics, Am, and fission product materials such as  $^{137}\text{Cs}$ . Upon completing the measurements, APMI performed a quality control check of the data, and returned to problem areas for further data acquisition. These activities produced the assay results from the data provided in this report. Table 1 shows the wells on which the demonstration was to be performed.

**Table 1. Information on Active Wells Logged by APMI**

<b>Well Identifier</b>	<b>Depth in Feet</b>	<b>Location</b>	<b>Element of Interest</b>
W10-69	40 to 45	West of T Tank Farm	Pu-239
W10-73	35 to 40	West of T Tank Farm	Pu-239
W15-82	66	Z-9 Area	High Chlorine



## Test Pits and Calibration Models

Table 2 and associated data, shown below, are the grade assays for the Hanford test pits. APMI ran the PNG in passive mode in the SBA and SBB test pits and the PFN in SBL and SBH test pits. Calibration of the tools is based on the values in this table.

### Hanford Calibration Models

model	depth, ft	<sup>40</sup> K (pCi/g)	<sup>238</sup> U (pCi/g)	<sup>232</sup> Th (pCi/g)	$\rho$ dry/wet	mR/hr
SBT	8.5	10.6 ± 1.3	10.02 ± 0.48	58.1 ± 1.4	1.92/2.15	0.298 ± 0.019
SBK	17.5	53.5 ± 1.7	1.16 ± 0.11	0.11 ± 0.02	1.82/2.07	0.0187 ± 0.0014
SBU	8.5	10.7 ± 0.8	190.5 ± 5.8	0.66 ± 0.06	1.90/2.14	0.760 ± 0.096
SBM	17.5	41.8 ± 1.8	125.8 ± 4.0	39.1 ± 1.1	1.87/2.12	0.664 ± 0.065
SBL	8.5	undetermined	324.0 ± 9.0	undetermined	2.25/2.44	1.351 ± 0.197
SBH	17.5	undetermined	3126 ± 180	undetermined	2.25/2.44	10.86 ± 1.09
SBA	8.5	undetermined	61.2 ± 1.7	undetermined	2.19/2.38	0.257 ± 0.037
SBB	17.5	undetermined	902.0 ± 27.0	undetermined	2.20/2.38	3.59 ± 0.45

All models are 48" high, with 4.5" dia uncased hole along axis. SBT, SBK, SBU, SBM, SBL, & SBH are 48" diameter. SBA & SBB are 60" dia  
Gamma dose rate estimates based on data collected Nov 2007 and May 2008

Stromswold, D.C. 1994; *Calibration Facilities at Hanford for Gamma-Ray and Fission Neutron Well Logging*; PNL-9958, Pacific Northwest Laboratory, Richland, July, 1994

Steele, W.D. & D.C. George, 1986; *Field Calibration Facilities for Environmental Measurement of Radium, Thorium and Potassium*; Report GJ/TMC-01 (2<sup>nd</sup> Edn), Bendix Field Eng., Grand Junction, Colorado

#### Conversions:

1 pCi/g <sup>40</sup> K	= 0.1195 wt % K	~ 0.255 $\mu$ R/hr	~ 0.0643 pCi/g eRa226
1 pCi/g <sup>238</sup> U	= 2.997 ppm eU	~ 3.96 $\mu$ R/hr	~ 1 pCi/g eRa226
1 pCi/g <sup>232</sup> Th	= 9.091 ppm eTh	~ 4.39 $\mu$ R/hr	~ 1.11 pCi/g eRa226

**Table 2. Hanford Calibration Test Pit Summary Data**

## Logging Tools

APMI developed a method of analyzing subsurface contaminants using nuclear probes during the SBIR. The method consists of using three probes to measure different aspects of the materials surrounding the probe holes. The first, the PFN, uses a technique called "differential die-away" to measure fissionable materials. PFN tools have been used commercially in the uranium logging industry for three decades. It is a neutron measurement that induces fission in the materials in the formation with thermal neutrons that follow a pulse of 14 MeV neutrons and detects epithermal energy neutrons arising from the fission. It is not specific to the species of atom that is fissioning; hence it cannot differentiate directly between uranium and plutonium. However, by measuring the background neutrons (source off), one may obtain

additional information about other sources of neutrons in the environment such as spontaneous fission from  $^{240}\text{Pu}$  or  $\alpha$ -n neutrons from  $^{241}\text{Am}$ . Both active and passive scan results are presented in the discussions in this report.

We ran the PFN tool in the SBL/SBH test well in order to calibrate to uranium. There had been no previous calibration of this tool. The PFN was then run in wells W10-69 and in W10-73 where plutonium had been reported in previous Stoller logs. We then used the Monte Carlo program, MCNP, to provide a cross-correlation to the uranium response in the open-hole test pits and its response in the cased-hole target wells. In addition, MCNP provided a cross correlation between the PFN uranium and plutonium responses in the cased target wells.

The second tool is the PNG which is comprised of a pulsed neutron source and a high purity germanium diode detector, the GMX detector. This tool can be run actively (neutrons on) and passively (neutrons off). It is well suited to measuring small amounts of chlorine in the formation. When measuring high concentrations the count rates begin to saturate as the concentration becomes greater than 2% or 3%, and the uncertainties in the measurement become very large. In addition to chlorine, this tool measures many other elements in the environment such as iron, silicon, magnesium, calcium, sulfur, and sodium. In passive mode it will also measure the natural and man-made radio elements.

The neutron generator used in the PNG tool was loaned to APMI from a project at the Idaho National Laboratory, and it was never fully functional. Its output dropped in a matter of an hour to an unusable level, and it would have to be rested for a few minutes and then re-started to produce enough intensity for a useful measurement. It was also quite noisy electrically, and it caused the resolution of the germanium detector to broaden. Most of the time this was acceptable; however there were instances where it was too broad to resolve certain closely spaced elemental peaks.

We ran the PNG passively in all the measurements we made. This included the test wells SBB/SBA to acquire an absolute efficiency calibration from the uranium daughters. We also ran in W10-69, W10-73, and W15-82. We ran the tool actively only in W15-82 because we had been informed that the latter had high levels of chlorine in it. We were told that neither of the other two monitor wells had significant chlorine.

The third tool was a PNC built using the neutron generator for the PFN but substituting a two-detector NaI scintillator detector package for the PFN's  $^3\text{He}$  detectors. It measures the neutron capture-cross section of the materials around the borehole. We exploit this capability by using this technique to determine high concentrations of chlorine (> 3%). The PNC tool was only run in well W15-82.

## **Discussion of Field Trip Activities**

APMI personnel arrived in Richland on Monday July 21, and two days were spent unpacking, checking and preparing the logging tools and surface equipment with help from Stoller personnel at their

laboratory. APMI personnel took on-site training on Tuesday July 22. Upon going to the site on July 23, the first Test Pit calibration runs were started. The Test Pit calibration wells were completed by the end of the next day, and the first active well with a plutonium plume W10-69 was started on Friday July 25. Over the weekend routine tool maintenance, such as cable and connector repairs, was performed at the Stoller laboratory. Well 10-69 was completed on Monday, July 28, and the second plutonium well W10-73 was started the next day. After completing well W10-73 on Thursday July 31, APMI moved to the Z-9 area to log well W15-82 which was suspected of having a carbon tetrachloride plume. This well was completed Friday and the equipment was returned to the Stoller laboratory and packed for shipment.

## Results

### *Passive Results for all wells*

Processing of the passive GMX data for Pu wells SBA/SBB, W10-73, W10-69 and W15-82 was performed using Canberra Genie 2000 analysis software and with specific worksheets created to handle these data. Analysis was done using peaks that were observed and identified by Genie's isotope identification procedure on an 1800 sec run in W10-73. This identification was done for one long 1,800 second spectrum, shown in Figure 1. Note, that the upper spectrum (figure 1a) is a detailed expansion of the region from 200 keV to 700 keV of the lower spectrum (figure 1b).

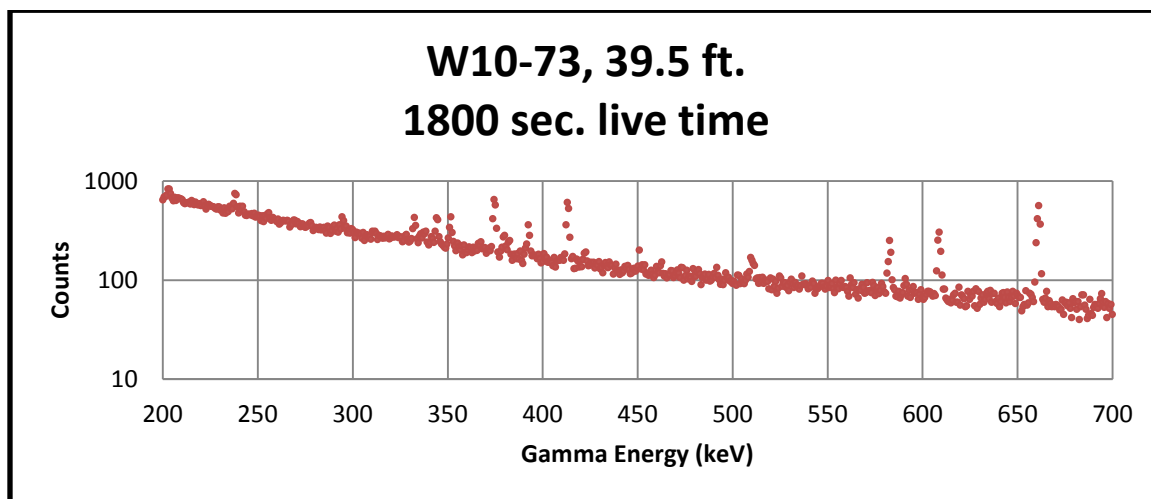
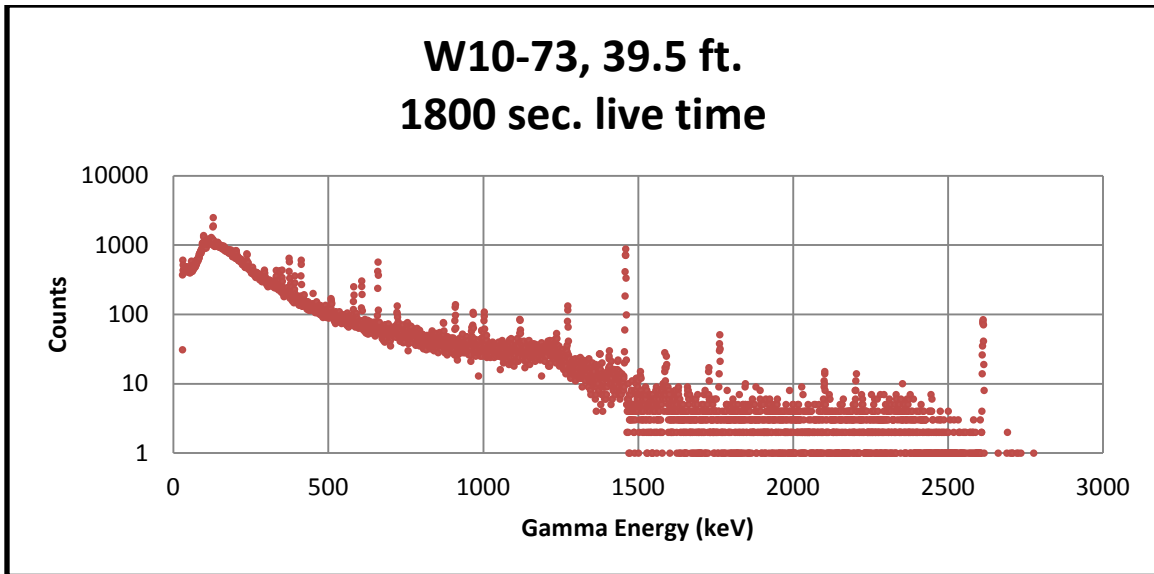


Figure 1a. Expanded passive gamma ray Spectrum with a 30 min accumulation time



**Figure 1b. Passive gamma ray Spectrum with a 30 min accumulation time**

The following  $^{239}\text{Pu}$  peaks were identified: 129.3, 203.6, 375.05, and 413.71 keV. The  $^{40}\text{K}$  peak at 1460.81 keV was present in every spectrum of W10-73 and W15-82; as was the 2614.53 keV peak from  $^{208}\text{Tl}$ . However; this was not true for W10-69. This lack of marker peaks, and much more gain and offset instability made the analysis of the W10-69 data more difficult.

The 661 keV peak from  $^{137}\text{Cs}$  and several gamma ray lines from  $^{154}\text{Eu}$  were observed.

Regions-of-interest (ROI) were set up for the  $^{239}\text{Pu}$ ,  $^{40}\text{K}$ , and  $^{137}\text{Cs}$  peaks, and Genie or Excel was used to determine the net peak areas and uncertainties for each peak in each station measurement. The  $^{154}\text{Eu}$  peaks were not processed to generate logs, although they could have been.

There was no measurable concentration of Pu or  $^{137}\text{Cs}$  in well W15-82.

### ***Passive Gamma Ray Logs in Test Pits SSA/SSB***

Data were acquired in the SBA/SBB calibration model to calibrate the PNG Passive measurement. This model has two zones with known concentrations of well equilibrated natural uranium. In our data there are 17 measurable peaks with known isotopic origin.

Using the published data<sup>4</sup> on branching ratios from these isotopes, the observed count rates were converted into efficiency, in cps/pCi, as a function of gamma ray energy, shown in Figure 2.

The efficiency is for the SBA/SBB borehole geometry which is air filled and has no casing. The borehole diameter, 4.5", is not much larger than the PNG pressure housing, so the hole-size effect should be small and is ignored. An attenuation correction is made to the calibration for steel casing in the monitor wells measured with PNG in Passive mode. No correction is needed for formation density.

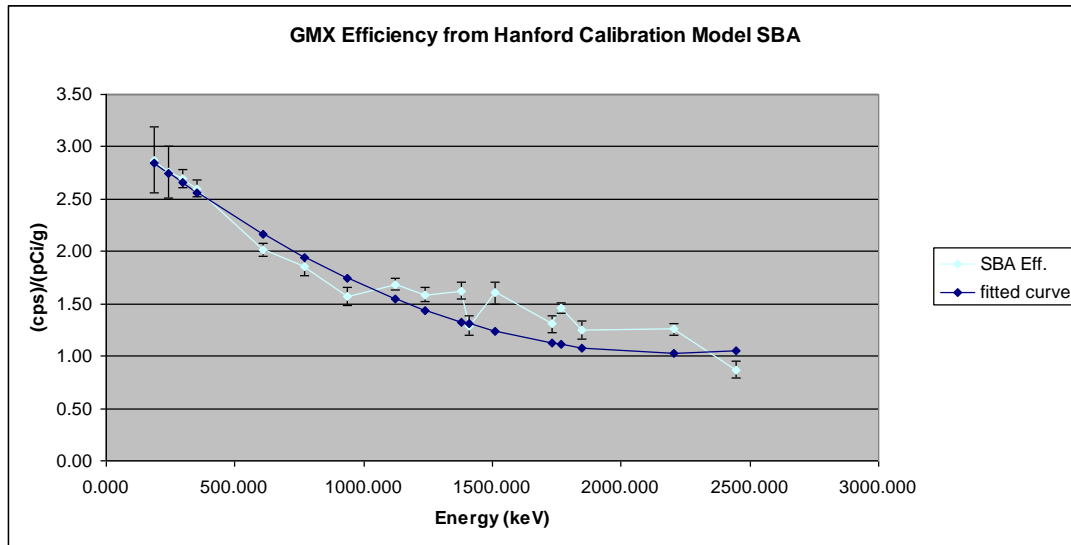


**Figure 2. Efficiency calibration. in 4.5" I.D. open hole air-filled geometry with density 2.38 g/cc using measurements in the SBA calibration model. To determine the activity, in pCi/g of a known isotopic source, divide the measured net peak counting rate of a gamma ray line from that source by the product of the efficiency and the branching ratio of the line, then apply any necessary borehole geometry corrections. The assumption is made that the radioactive material is distributed uniformly in the measured formation.**

Numerous gamma rays, mostly from <sup>214</sup>Bi, are emitted with known activity. Examples of the net peak count rates vs. depth for several such gamma ray lines are shown in Figures 3 through 6.

The measurement dead time in the lower zone, SBB, was more than 50%, so these data were not used for the calibration.

<sup>4</sup> National Nuclear Data Center, US Department of Energy, Brookhaven National Laboratory, <http://www.nndc.bnl.gov/>

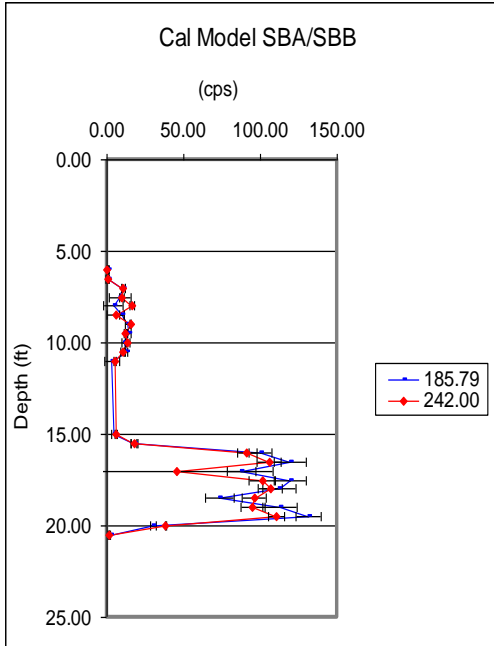


**Figure 3. Count rate vs. depth in SBA/SBB calibration model.**

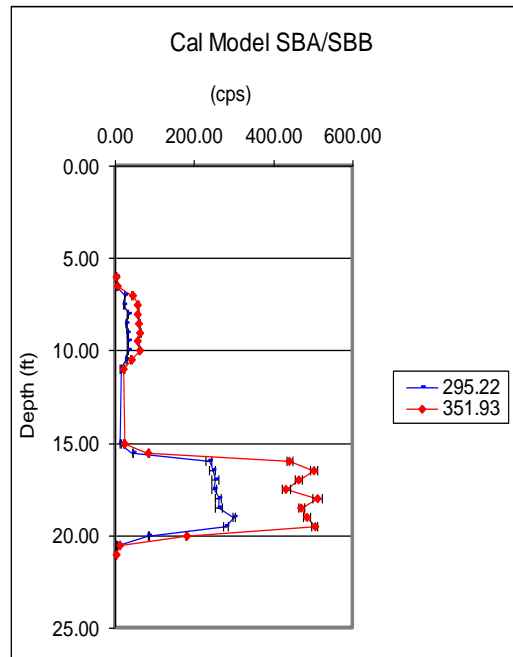


**Figure 4. Count rate vs. depth in SBA/SBB calibration model.**

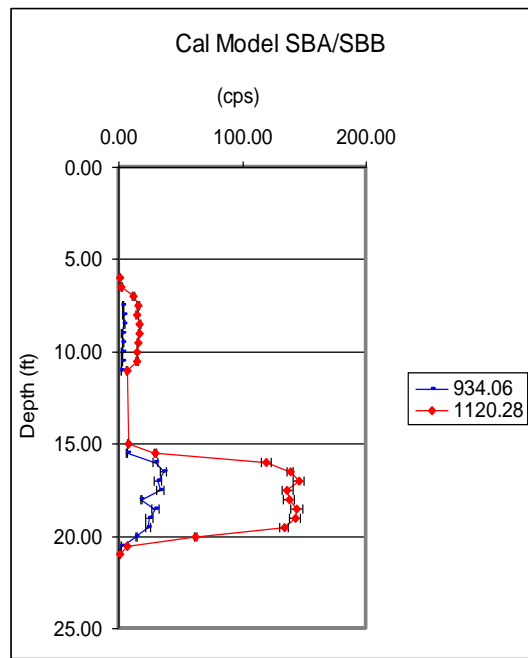
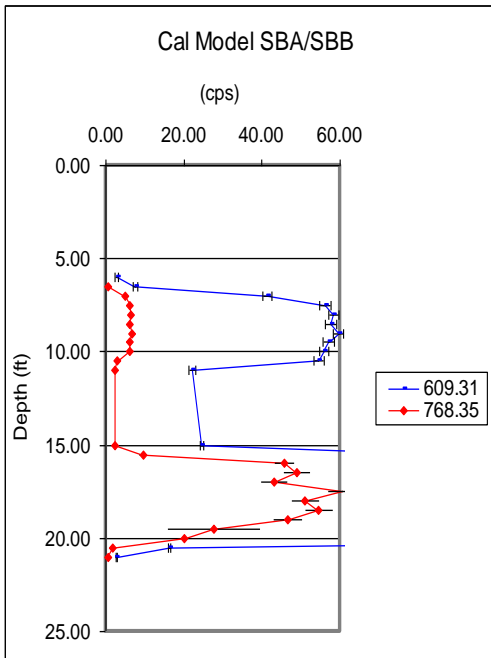


**Figure 5. Count rate vs. depth  
in SBA/SBB calibration model.**

**Figure 6. Count rate vs. depth in  
SBA/SBB calibration model**

**PFN Scans at the SBL/SBH Test Pits**

The PFN tool was operated in the SBL/SBH pit. In order to get into the pit, the top of the cover shield was removed because it was not aligned exactly with the borehole, and the tool diameter is 4.25 inches, thus not allowing much clearance. Data from this well, shown in Table 3 and Figure 7 are highly precise because the counts were taken for 5-minutes.

**Table 3. Results from the SBL/SBH measurements:**

Zone	Depth (ft from top of casing shield)	Counts per second per monitor count <sup>5</sup>	Assigned grade (ppm uranium)
Top	9 – 11	25.3	971
Bottom	20 – 18.5	247.6	9,368

These data are used to form the basic calibration of the PFN tool that was used to quantify the plutonium response in wells W10-69 and W10-73. The log in Figure 7 shows the scan of the test pit taken at 6-inch intervals. The depth indication is relative to the bottom bull nose of the PFN tool. Because the well cap was removed, there is an offset in the depth of the active zones in the well.

---

<sup>5</sup> An extra set of thermal neutron detectors is included in the tool design, and the counts from the thermal neutrons are used to normalize the epithermal fission neutron counts. These thermal detectors compensate for the effects of the downhole environment on the neutrons that cause fission.

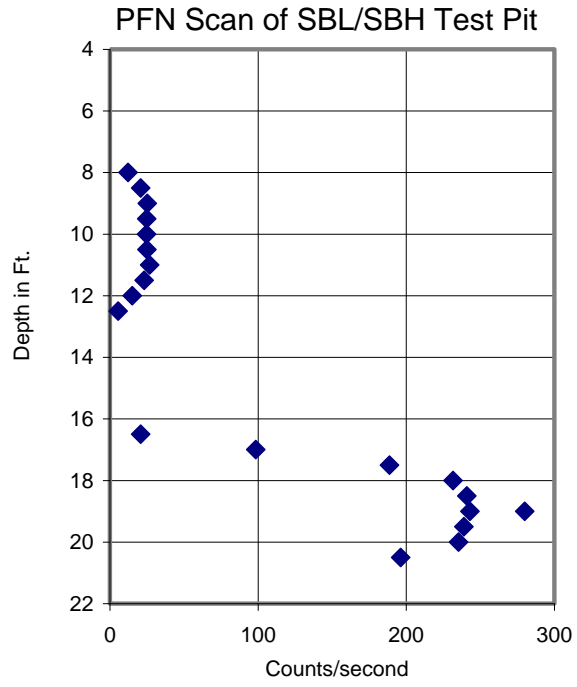


**Figure 7. PFN Log of the SBL/SBH test pit. Results are presented in counts/second**



# Plutonium Plume Well W10-69

## Passive Gamma Ray logs from Well W10-69

Four  $^{239}\text{Pu}$  gamma rays, 129.3-, 203.6-, 375.1-, and 413.7-keV, were measured in this well. The latter two gamma ray lines have better statistics and are less subject to interference, so these two are used for creating logs. See Figure 8.

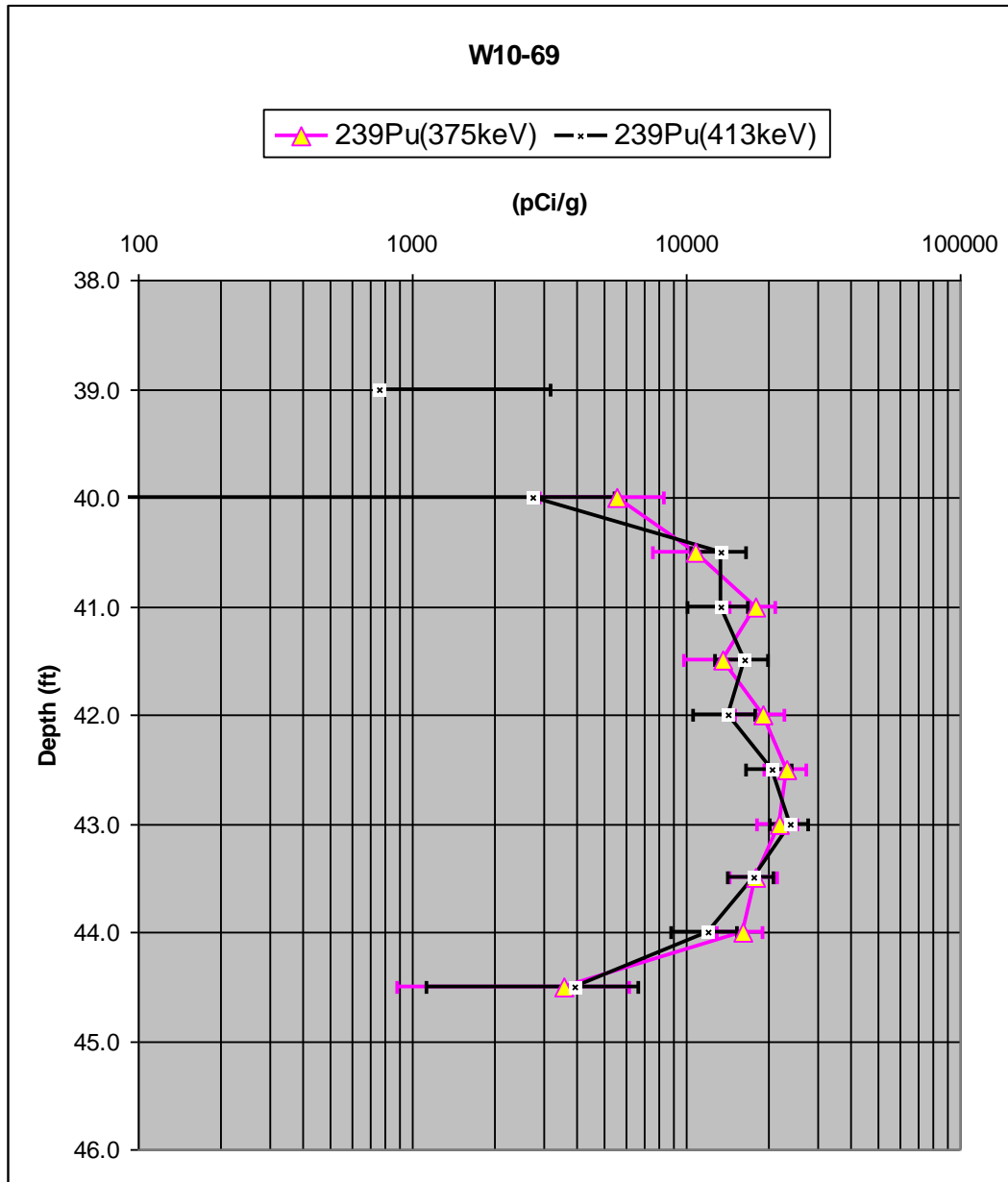


**Figure 8. Passive scan of the Pu 413 line in W10-69. The logarithm scale is used to show variation over a significant range of concentration**

The 661.66 keV peak from  $^{137}\text{Cs}$  was seen frequently. We investigated the amount of interference from the 662.4 keV line from  $^{241}\text{Am}$ . Because of the counting times selected, the statistics limited the precision of the 6-inch spaced station measurements. Hence, data from six station measurements at depths from 40.5 through 43.0 feet were summed for the interference analysis. (To do this, it was necessary to energy calibrate and re-bin the station measurements.) The summed range spans the depth where Pu activity was largest, as shown in Figure 8. In the summed spectrum, peaks were seen at 661.79, 723.3, 996.13, 1004.95, and 1274.81 keV, amongst other lines. These peaks correspond to known lines at 661.65 ( $^{137}\text{Cs}$ ) and  $^{154}\text{Eu}$  lines at 723.3, 996.26, 1004.72, and 1274.43 keV. For the summed spectrum the energy calibration derived from other known lines has a measured bias of  $0.16 \pm 0.13$  keV. The energies of the  $^{241}\text{Am}$  lines at 662.4 and 722.01 keV differ from the observed peaks by 0.61 and 1.29 keV, respectively, and the peak energies differ from the  $^{137}\text{Cs}$  and  $^{154}\text{Eu}$  lines by 0.01 and 0.00 keV, so it is unlikely that  $^{241}\text{Am}$  is a large contributor to these peaks.

A method previously used by Sotller to determine  $^{241}\text{Am}$  in this well was used to estimate the  $^{241}\text{Am}$  fraction in the 723.30 keV peak. The net peak counts and  $^{154}\text{Eu}$  branching ratios for the 1274.43 and 723.30 keV lines were used to compute the excess of counts in the 723.30 keV peak, assuming that there is no interference in the 1274.81 keV peak. The excess counts were then used to calculate the  $^{241}\text{Am}$  activity. As pointed out by Stoller, this calculation “is qualitative.” It is heavily influenced by statistical uncertainties and accuracy of branching ratios. One can then, using the  $^{241}\text{Am}$  activity and branching ratios for its 662.4 and 722.01 keV lines, compute the  $^{241}\text{Am}$  counts in the 661.79 keV peak. The result for the summed spectrum is that the  $^{241}\text{Am}$  contribution is  $13 \pm 3\%$  of the peak counts. The APMI  $^{137}\text{Cs}$  logs were not corrected for this interference.

It should be noted, as shown in Table 4 that the APMI  $^{137}\text{Cs}$  log attains a peak value about 5 times that of the Stoller log. To explain this difference as interference, about 80% of the 661.79 keV peak would have to be from  $^{241}\text{Am}$ . This would surely change the apparent energy of the peak (and that is not observed), and the qualitative analysis indicates only a 13% effect

Logs for  $^{137}\text{Cs}$ ,  $^{40}\text{K}$ , and  $^{208}\text{Tl}$  are shown in Appendix B. The APMI data would allow creation of a  $^{154}\text{Eu}$  log; however, the data do not support a  $^{241}\text{Am}$  log.

Conversion of the observed net peak count rates for  $^{239}\text{Pu}$ ,  $^{137}\text{Cs}$ ,  $^{40}\text{K}$  and  $^{208}\text{Tl}$  to pCi/g was done as described in the caption to Figure 2. No correction was made for borehole size, since this is negligible<sup>6</sup> for an air filled borehole. A correction was made for attenuation by the 5/16” steel casing. The mean-free-path of gamma rays in iron used for the attenuation correction in the steel casing is shown in Figure 9.

---

<sup>6</sup> “Open Hole Gamma Ray Corrections”, Schlumberger

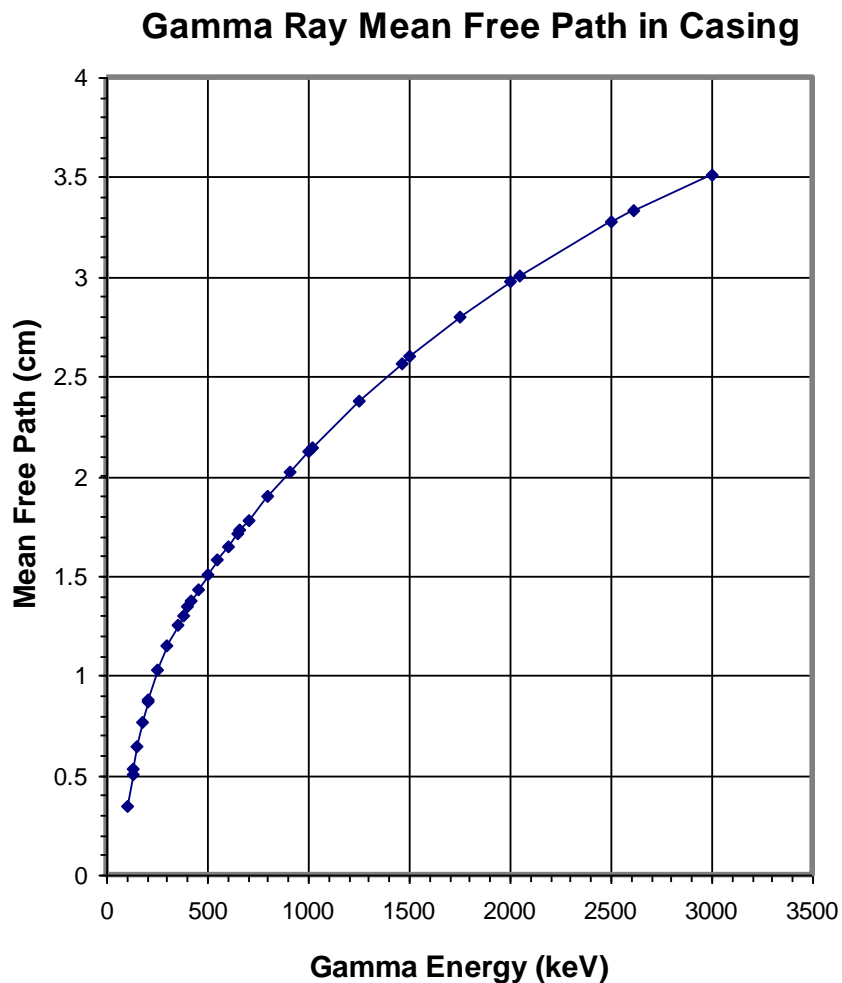


Figure 9. Mean free path of gamma rays in Fe<sup>7</sup>

### *PFN Log of Well W10-69*

Figure 10 shows the PFN log of well W10-69 taken at 6-inch intervals. The statistical uncertainties in the data are comparable with the marker size. Based on the count rates in the low activity areas, we estimate that the MDL for Pu detection is approximately 1.5 nCi/gm.

<sup>7</sup> “Tables and Graphs of Photon Interaction Cross Sections from 1.0 keV to 100 MeV Derived from the LLL Evaluated Nuclear Data Library”, Plechaty, E.F., Cullen, D.K., and Howerton, R.J., UCRL-50400.

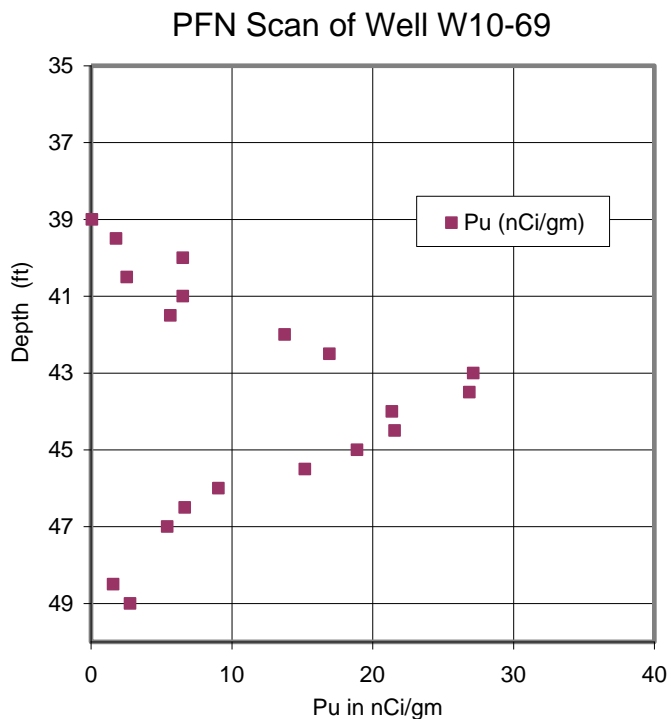


Figure 10. PFN Scan of Plutonium in Well W 10-69

## Plutonium Plume Well W10-73

### *Passive Gamma Ray Logs*

The calibration from SBA (Figures 3 to 6.) and the effects of Fe-casing attenuation (Figure 9) were used to convert the count rate logs to pCi/g. No correction for borehole size was made since air borehole corrections are very small.

An analysis for interference of  $^{241}\text{Am}$  in the 662 keV peak was made as described in the section, "*Passive Gamma Ray logs from Well W10-69.*" For W10-73, the 1800 second station measurement at measurement depth 39.5 ft., shown in Figure 1, was used. The result for the  $^{241}\text{Am}$  contribution to the 662 keV peak is negative,  $-2.1 \pm 4.6\%$ . There is no indication in our data that  $^{241}\text{Am}$  contributes significantly to the peak. For this well, the APMI and Stoller logs for  $^{137}\text{Cs}$  are in good agreement, as shown in Table 4.

The results from the Pu lines at 129.3-, 203.6-, 375.1-, and 413.7-keV gave consistent results. Logs for 375.1-, and 413.7-keV are shown in Figure 11. Logs for  $^{137}\text{Cs}$ ,  $^{40}\text{K}$ , and  $^{208}\text{Tl}$  are shown in Appendix B.

# W10-73

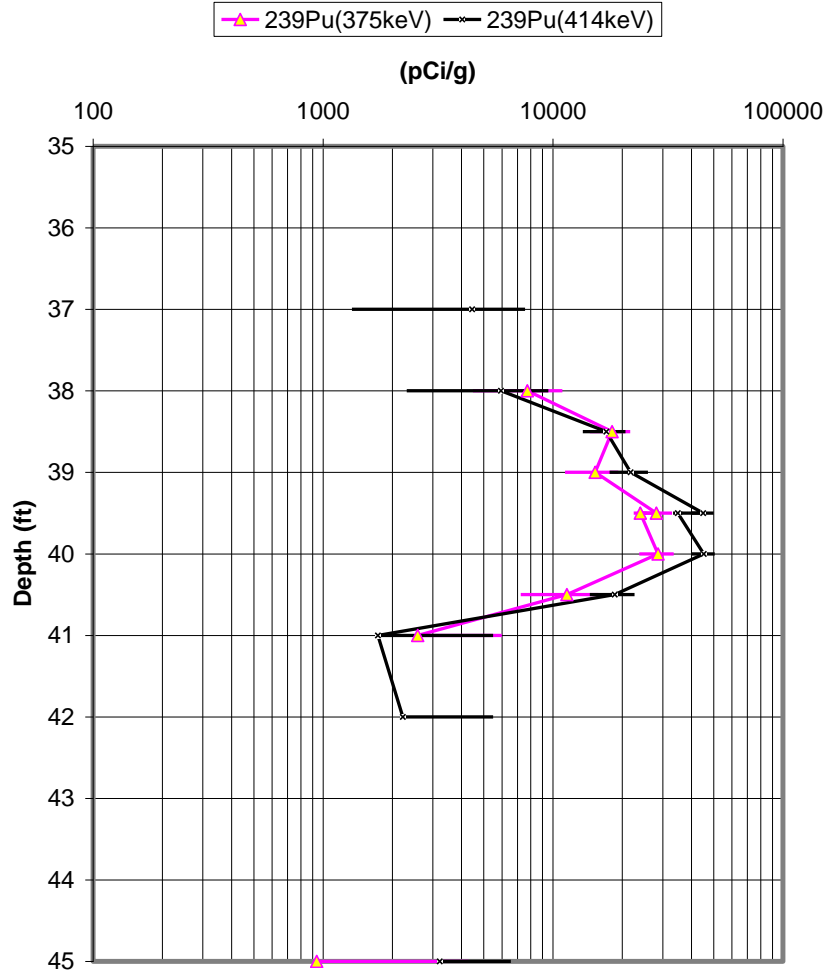


**Figure 11.  $^{239}\text{Pu}$  logs from W10-73**

***PFN Log in Well W10-73***

Figure 12 shows the PFN scan of well W10-73. Statistical uncertainties are approximately equivalent to the size of the markers. The very low level fissionable response (e.g. less than 10 nCi/gm) may either be Pu or background uranium. At those levels, it would take longer measurements to differentiate the

plutonium and uranium contribution to the signal. We investigated the background neutron signals coming from spontaneous fission and from ( $\alpha,n$ ) reactions from Am and Pu. There is no significant evidence for these background contributions in W10-69 and W10-73. The points plotted in Figure 12 are the total count for a 5 minute data point. The Pu concentrations are based on counts/second. Thus the background is a very small fraction of the signal, and it is difficult to make any assertions about the causes of the background from such a poor signal. The most general statement that could be made is that the background counts appear to have the same structure vs. depth in both wells. That is expected as both wells penetrate the same strata.

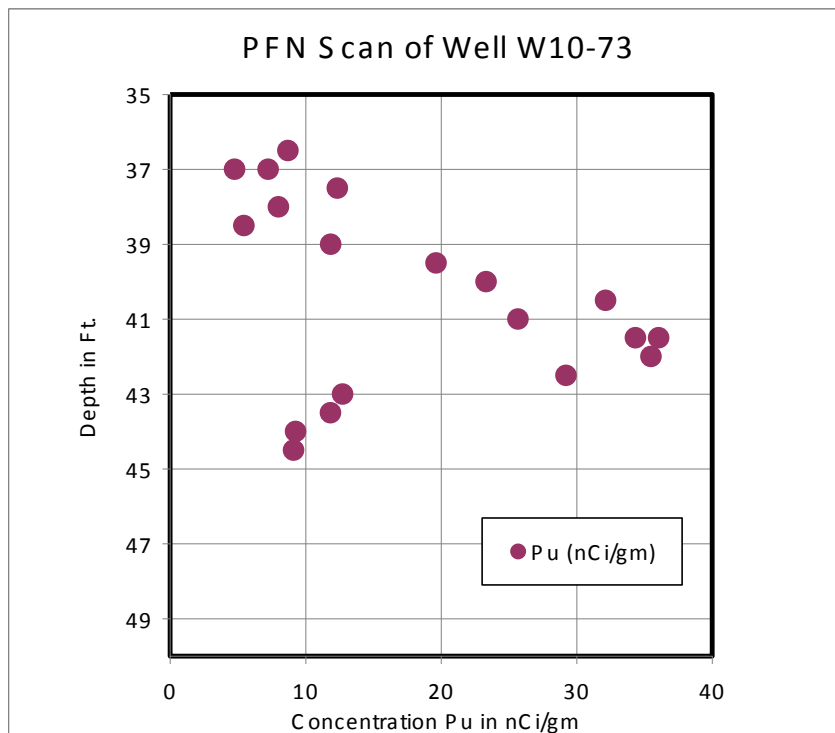


**Figure 12. PFN scan of well W10-73**

Comparison with the S. M. Stoller Corp. values in the range of overlap, 39 – 45 ft, is given in Table 4. The Pu (nCi/g) values are averages of the 375- and 414- keV logs at the depth of highest log values, 43 ft for W10-69 and 40 ft for W10-73. These data also show the comparison to the PFN results. It is clear that there is a significant difference in the Pu concentrations between the PFN log and the Stoller log in well W10-73. We believe it is significant that both the APMI gamma logs and the PFN logs show similar results between wells W10-69 and W10-73 while the Stoller log in W10-73 is predicted to be almost twice as high as the PFN and APMI gamma log. Additional measurements may be needed to resolve this issue.

**Table 4. Comparison of W10-69 and W10-73 results from gamma and neutron measurements.**

Well ID:	W10-69	W10-73
----------	--------	--------

Logged by:	APMI Gamma	APMI PFN	S. M. Stoller Corp.	APMI Gamma	APMI PFN	S. M. Stoller Corp.
Date of log	7/25/08	7/27/08	5/31/06	7/28/08	7/29/08	6/05/06
Depth of Pu zone (ft)	40.5 – 44.0	41 – 47	41-43	39.0 – 40.5	39 – 45	39-40
Maximum <sup>239</sup> Pu (nCi/g)	23 ± 0.5	27.1	28	37 ± 0.8	36	63
Depth of <sup>137</sup> Cs zone (ft)	40.5 – 43.0		41-42	38.5 – 45.0		39-41
Maximum <sup>137</sup> Cs (pCi/g)	1.0		0.22	0.93		0.9
Maximum <sup>40</sup> K (pCi/g)	15.		17	20		19
Maximum <sup>208</sup> Tl (pCi/g)	0.4		0.7	0.35		0.6

## Well W15-82

### Passive Gamma Ray Logs

There was no measurable concentration of Pu or <sup>137</sup>Cs in well W15-82. Figure 13 shows a log made from the sum of the 375.1-, and 413.7-keV Pu lines, to improve statistics. Note that the line extending to 170 nCi/g at 58 ft is a large error bar. The log value is 25 nCi/g. None of the log values are more than two standard deviations from zero. Logs for <sup>40</sup>K and <sup>208</sup>Tl are shown in Appendix B. Logs for <sup>40</sup>K and <sup>208</sup>Tl are shown in Appendix B.

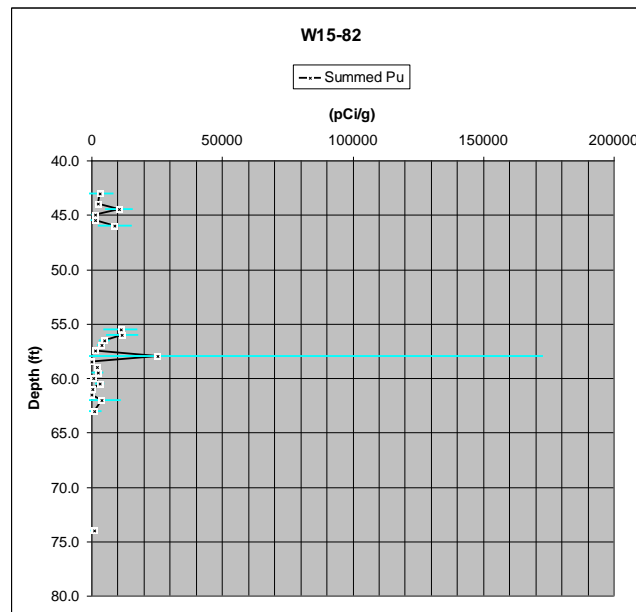
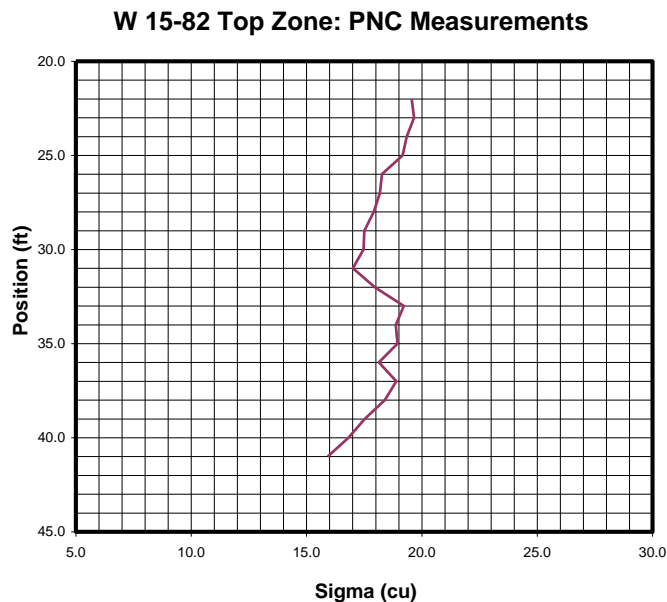


Figure 13. <sup>239</sup>Pu log for W10-82. <sup>239</sup>Pu is not measurable in these data.



### Neutron Decay Time Measurement Logs

The neutron capture cross section, sigma, from the PNG tool is shown below in Figures 14 and 15. Two zones were logged in an attempt to see if large concentrations of carbon tetrachloride were present. Pure CCl<sub>4</sub> has a capture cross section of 821.6 capture units (cu)<sup>8</sup>, and therefore if only 5 porosity units (pu)<sup>9</sup> of the pore space were filled with CCl<sub>4</sub> it would cause an increase of sigma by 41 cu. No such change in sigma was observed, but there are localized zones with changes (in the top and bottom zones: see logs below) that possibly could be due to very small amounts of CCl<sub>4</sub>, or due to changes in formation lithology and the effects of moisture. Such interpretation scenarios can be easily evaluated, but are beyond the scope of this report. Water has a capture cross section of 22 cu.



**Figure 14. Top Zone Sigma Measurement**

<sup>8</sup> CU or capture units are measures of neutron interaction probabilities. A capture unit is equal to 1/1000 of an inverse centimeter (cm<sup>-1</sup>), the usual unit used in neutron physics.

<sup>9</sup> PU or porosity unit is the volume fraction of void space assigned to pores in rocks. A PU is expressed as a percent. In the present case, 5 pu refers to the amount of the total volume filled with water in the vadose zone.

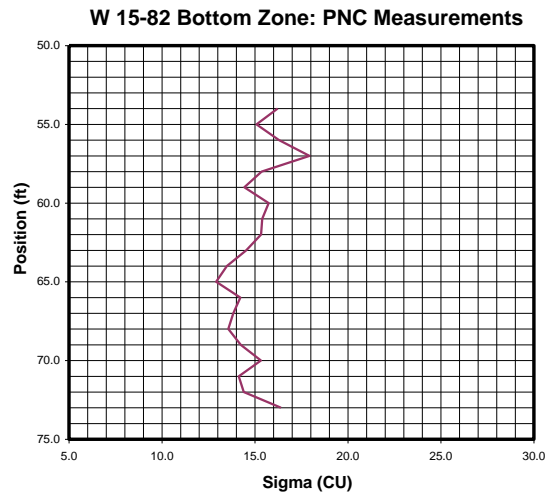


**Figure 15. Bottom Zone Sigma Measurement**

### *Chlorine Capture Logging*

The PNG tool and the PNC tool together represent a means of quantifying chlorine concentrations over a wide range of values. The PNG is best suited for low concentrations, and the PNC is best suited for high concentrations. In W15-82 there were only low chlorine concentration values. Hence, the PNC tool added little to the understanding of the results in this well.

The PNG tool was run in capture-mode at 11 stations in this well. The result, a log scan, of the two most intense peaks is shown in Figure 16. The logging spectral measurements with highest chlorine yields in the upper and lower regions of the well were summed to provide better statistical precision.

The Cl log uses the thermal neutron flux at the HPGe detector, measured by the 1096 keV gamma ray from <sup>70</sup>Ge capture to normalize both the calibration data and the log data. This has the benefit of canceling dead time and neutron generator output changes.

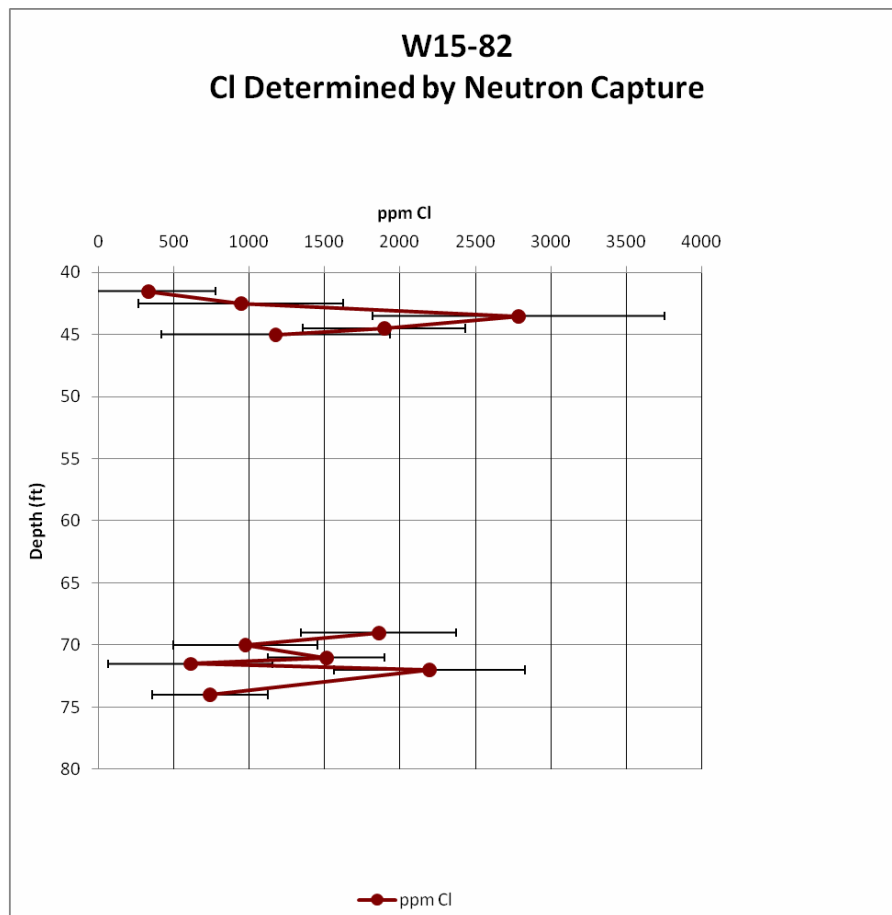
The calibration data were for a 5-inch I.D. casing with 0.5-inch wall thickness. The well data were for an 8-inch I.D. casing with 5/16- inch wall thickness. Correction to the gamma ray signal was made for the different iron attenuation, and the borehole size effect on gamma ray tools in an air borehole is small. However; the effect of the different casings may not be negligible on the thermal neutron normalization. This could be evaluated with MCNP, but is beyond the scope of the present contract.

Table 5 shows the statistical analysis of the data and which points are the most credible from a statistical basis. Columns 4 and 5 show the counts resulting from subtraction of one and two standard deviations (respectively) from the nominal value. Any case where the 2-sigma limit is less than zero should be

suspect, and a case where the one-sigma limit is negative does not represent a viable datum. Column 6 is our evaluation of the measurement.

The PNC log values were used to estimate the potential contribution from chlorine to SIGMA. The right hand column (8<sup>th</sup> column) shows the contribution to the total capture cross section (7<sup>th</sup> column) from the imputed chlorine concentrations. As can be seen, this is a very small fraction of the total cross section, and hence the capture cross section measurement does not contribute to understanding the amount of chlorine present in this well.

Spectral measurements in the two highest zones of chlorine, shown in Figure 16, were summed to enhance their statistical precision. These data are extremely useful. First, by summing the spectra, we obtained definite evidence for more than the two strongest Cl lines used in the logging scans. The additional chlorine peaks confirm the analysis. Second, a 6.129 MeV line near the slightly lower energy Cl line is almost certainly due to oxygen activation, which will not appear in most data bases. Third, the summed spectra shows lines from other elements, some of which have been found in the activation spectra, e.g. Mn. This gives greater confidence in the other results.



**Figure 16. Cl log from PNG Capture measurement.** The log, red, with one standard deviation error bars is from the sum of the 788- and 1165-keV peaks.

**Table 5. Computed Capture Cross Sections using Chlorine Capture Concentrations**

Depth Ft	PPM Chlorine	Standard deviation in ppm Cl	Cl -1 SD	Cl - 2 SD	Evaluation	Total SIGMA	SIGMA from Cl
41.5	329	448	-120	-568	NO	17.2	0.3
42.5	944	681	263	-419	SUSPECT	15.9	0.9
43.5	2787	968	1819	850	LIKELY	NM	2.5
44.5	1896	538	1357	819	LIKELY	NM	1.7
45	1174	757	416	-341	SUSPECT	NM	1.1
69	1858	515	1343	827	LIKELY	13.6	1.7
70	973	477	496	19	LIKELY	14.2	0.9
71	1511	385	1126	741	LIKELY	15.3	1.4
71.5	610	544	66	-478	SUSPECT	14.7	0.6
72	2196	632	1563	931	LIKELY	14.1	2.0
74	738	384	354	-31	SUSPECT		0.7

## General Discussion of Other Elemental Capture and Activation Data from PNG

Looking at capture spectra, there are observable peaks from Al, Si, Fe, Ca, and probably Ti. There is no evidence of sulfur. With a short campaign of tool characterization measurements, it is straightforward to differentiate iron in the casing from iron in the formation. There are a number of other apparently statistically significant peaks that could not be quickly identified without a significant amount of additional work or examining all the capture spectra outputs in much more detail than is warranted at this point. However, this does seem to indicate that we can quantify a broad suite of elements that would provide a useful description of the geological environment.

A quick examination of the activation results show information on the following elements:

1. Magnesium (843.8 keV, 9.45 min) is clearly present
2. Sodium (2754 and 1368.6 keV, 15 hour) is clearly present
3. Aluminum (1777.8 keV, 2.25 min) is clearly there, however there is weak evidence for the presence of <sup>29</sup>Al (1273.2 keV, 6.5 min) from the <sup>29</sup>Si(n,p) reaction so a quantitative analysis of the amount from Al would require a more detailed analysis

4. Manganese (1810.7 keV, 2.6 hour) is clearly present
5. There is some definite evidence for the presence of vanadium (1434.2 keV, 3.76 min).
6. There is no evidence for the presence of calcium (3084 keV, 8.72 min) as an activation product. This is expected in a non-carbonate environment because of the weak activation properties of Ca.
7. Evidence for chlorine (2167.6 and 1642.2 keV, 37.2 min) in the activation spectra is weak, as expected from the apparent concentrations observed in the capture measurements
8. There are also some other lines present that could be due to unidentified elements, natural activity, or transuranics.

## Conclusions

The following inferences can be gained from this work:

- The PFN is able to measure extremely small amounts of Pu with high precision and accuracy behind casing. In environments with high levels ( $> 100$  nCi/gm) of Pu, measurement times could be as short as one minute. Where high precision is needed on very low concentrations (e.g.; less than 10 nCi/gm), 5-minute station measurements will provide useful answers.
- Well #W15-82 was expected to contain significant amounts of chlorine, however, the PNG measurement showed that the amount of chlorine present was less than 2,700 parts per million. The PNC measurement did not contribute to the measurement for such low concentrations: it is a tool for observing high concentrations, e.g.; greater than 3% chlorine.
- There is a significant difference in the Pu concentrations between the PFN log and the Stoller log, recorded in June 2006, in well W10-73. We believe it is significant that both the APMI gamma logs and the PFN logs show similar values in wells W10-69 and W10-73 while the Stoller log in W10-73 shows almost twice as high a concentration as the PFN and APMI gamma log. It would be useful to perform additional measurements in this well to address this discrepancy.
- The PNG is a valuable tool to identify small amounts of chlorine in downhole environments. With a more functional neutron generator, these measurements can be done quickly and accurately.
- The application of the PNC for use in high chlorine environments was developed to eliminate the effects of count rate saturation that prevent neutron spectroscopy tools from performing accurate measurements at concentrations above a few tens of thousands of parts-per-million of chlorine. It is not useful for measuring small concentrations, and there were no areas of high concentrations in the set of holes we logged. The discussion on pages 15 *et seq.* is an attempt to illustrate how this tool could be used fruitfully in a more interesting environment.

APMI will be happy to address any questions or comments concerning this work both by phone and by a visit to Richland in the near future.

J. S. Schweitzer helped with PNG post-logging analysis. We enjoyed working with James Meisner, Melinda Holloway, and Alan Pearson of the S. M. Stoller Corporation. Scott Petersen, Tracey Burch, Kimball Smith, and other Fluor Hanford personnel helped us get this work under way, and we appreciate their help to complete this project.

# **APPENDIX A: Previous measurements and summary of Hanford wells**

## **Previous Data**

The Hanford Site covers approximately 586 square miles. Past nuclear weapon production activities at the Site resulted in approximately 1.7 trillion liters (450 billion gallons) of liquid waste being released to the ground. Much of the associated contaminants remain in the vadose zone, between the top of the water table and the surface, but some have reached the groundwater. Hazardous chemical contaminants include carbon tetrachloride, chromium, and nitrates. Radioactive contaminants include iodine-129, strontium-90, technetium-99, tritium, and uranium.

The U.S. Department of Energy, the U.S. Environmental Protection Agency, and the Washington State Department of Ecology have developed a remediation plan for protecting the Columbia River Corridor. The Groundwater Remediation Project is largely responsible for ensuring the plan is implemented.

The Central Plateau Closure Project was established to plan and execute the regulatory and technical activities necessary to enable cleanup decisions to be made for the Hanford Site's Central Plateau waste sites and structures. In accordance with the Hanford Federal Facility Agreement and Compliance Order (Tri-Party Agreement), Comprehensive Environmental Response, Compensation, and Liability Act (CERCLA) processes are the primary decision drivers for cleanup of most of the waste sites, in conjunction with Resource Conservation and Recovery Act (RCRA) closure processes where applicable.

As part of the CERCLA process, multiple remedial investigations (RI) and feasibility studies (FS) are conducted on operable units within the Central Plateau. The signatories to the Tri-Party Agreement – the U.S. Department of Energy (DOE), the U.S. Environmental Protection Agency (EPA), and the State of Washington Department of Ecology (Ecology) – have agreed to changes to RI/FS activities to enable more effective decisions on remedial actions for the Central Plateau. This process has already included evaluating critical parameters affecting the RI/FS process, and continues in evaluating a more streamlined and consistent approach to develop and evaluate project uncertainties regarding this same decision making.

As a result, APMI agreed to conduct geophysical logging in wells W10-69, W10-73, and W15-82. The depth, location, and element of interest for each well is shown in Table 1.

### **Well W10-69**

Previous data on well 299-W10-69 (A7159) were obtained from the S. M. Stoller Corp. report HGLP-LDR-013 dated 10/10/06. Excerpts from this report are repeated below along with selected logs:

## **Results and Interpretations:**

*Manmade radionuclides detected in this borehole included  $^{239}\text{Pu}$ ,  $^{241}\text{Am}$ ,  $^{137}\text{Cs}$ , and  $^{154}\text{Eu}$ .*

*Full energy peaks attributed to  $^{239}\text{Pu}$  are detected at 375.05 and 413.71 keV. The 375.05 keV gamma ray has a slightly higher yield and is used to assay the  $^{239}\text{Pu}$ .  $^{239}\text{Pu}$  is detected between 39 and 42 ft with a maximum concentration of approximately 29,000 pCi/g at 42 ft.*

*$^{241}\text{Am}$  is detected from 39 to 44.5 ft with a maximum concentration of approximately 54,000 pCi/g. This assay should be considered qualitative.  $^{241}\text{Am}$  is usually assayed using the 662.40 or 722.01 keV energy peaks. In this borehole, interferences are occurring from  $^{137}\text{Cs}$  (661.66 keV) and  $^{154}\text{Eu}$  (723.31 keV). The influence from  $^{154}\text{Eu}$  was subtracted from the 722.01  $^{241}\text{Am}$  energy peak to determine the concentration of  $^{241}\text{Am}$ .*

*Residual counts attributed to  $^{241}\text{Am}$  in the 662 keV energy peak were subtracted to provide a  $^{137}\text{Cs}$  assay. It is estimated the maximum  $^{137}\text{Cs}$  concentration is approximately 0.25 pCi/g.*

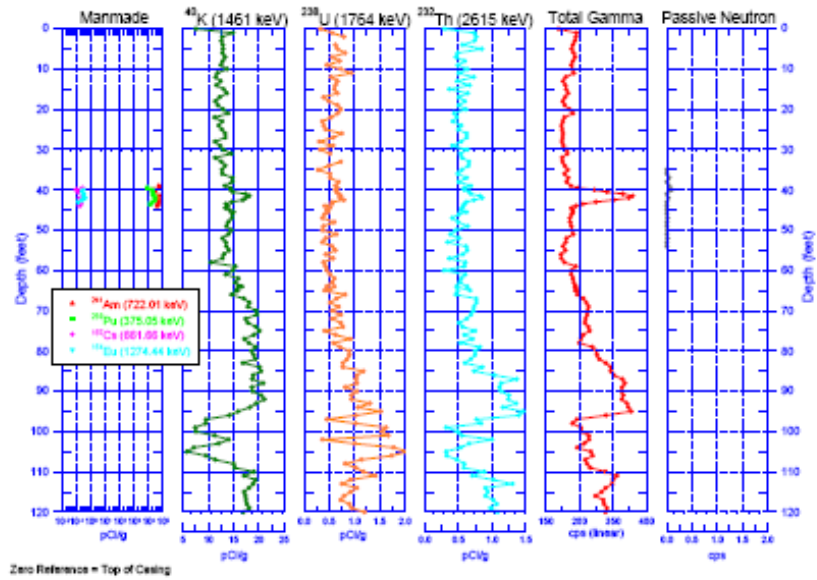
*$^{154}\text{Eu}$  concentrations were determined from the 1274.44 keV energy peak. The 723.31  $^{154}\text{Eu}$  gamma line is also observed in the spectra but exhibits less yield than the 1274.44 keV gamma line.  $^{154}\text{Eu}$  is detected from 40 to 43 ft with a maximum concentration of 0.3 pCi/g.*

*Passive neutron logging was performed in the borehole. This logging method has been shown to be effective in qualitatively detecting zones of alpha-emitting contaminants from secondary neutron flux generated by the ( $\alpha$ ,n) reaction and may indicate the presence of  $\alpha$ -emitting nuclides, including transuranic radionuclides, even where no gamma emissions are available for detection above the MDL. The passive neutron signal depends on the concentration of  $\alpha$  sources, and also the concentrations of lighter elements such as N, O, F, Mg, Al, and Si which emit neutrons after alpha capture. The passive neutron log indicated a maximum count rate of approximately 0.1 counts per second (cps) at 40 ft. Although very small, the presence of any neutron flux is an indication of transuranic waste.*

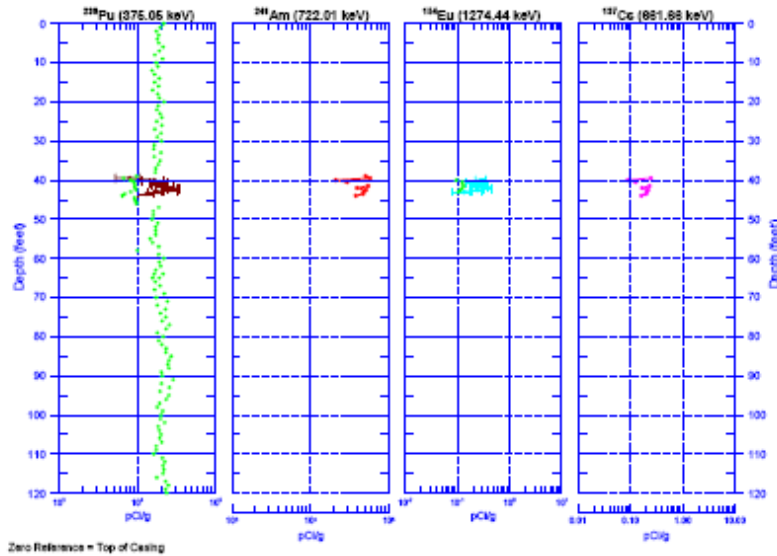
*The SGLS repeat sections of natural gamma logs show good repeatability. The manmade radionuclides do not show repeatability. The data acquired at 400 second counting times at 0.5 ft intervals show more detections than the data acquired at 100 seconds at one ft intervals. The lack of detections in the 100 second data suggests the system is very near the minimum detection level at that counting time.*



299-W10-69 (A7159) Combination Plot



299-W10-69 (A7159) Manmade Radionuclide Plot



**Well W10-73**

Previous data on well 299-W10-73 (A7163) were obtained from the S. M. Stoller Corp. report HGLP-LDR-036 dated 11/22/06. Excerpts from this report, that differ from the previous report on Well W 10-69, are presented below along with selected logs:

**Results and Interpretations:**

<sup>239</sup>Pu is detected from 37.5 to 40 ft with a maximum concentration of approximately 62,000 pCi/g at 39.5 ft.

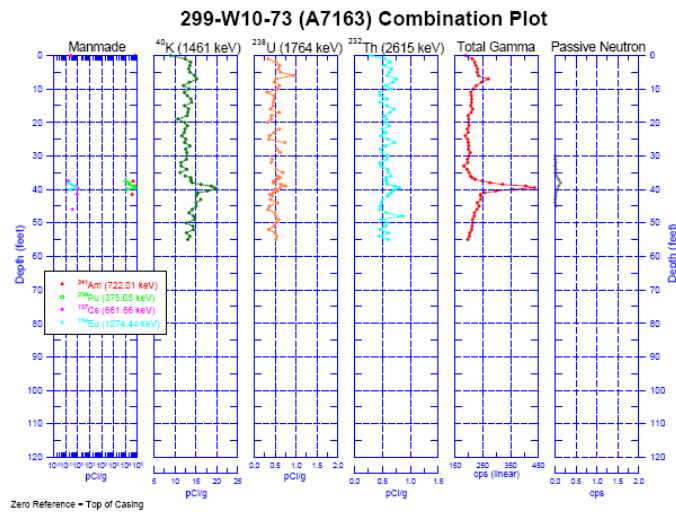
<sup>241</sup>Am is detected at 37.5, 39 to 40, and at 41.5 ft with a maximum concentration of approximately 64,000 pCi/g at 39.5 ft. This assay should be considered qualitative.

Residual counts attributed to <sup>241</sup>Am in the 662 keV energy peak were subtracted to provide a <sup>137</sup>Cs assay. It is estimated the maximum <sup>137</sup>Cs concentration is approximately 0.7 pCi/g.

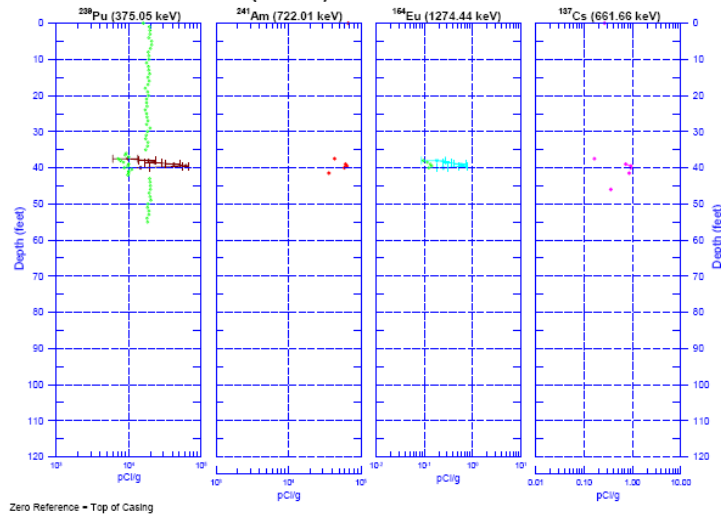
<sup>154</sup>Eu is detected from 38 to 40 ft with a maximum concentration of 0.8 pCi/g.

The passive neutron log indicated a maximum count rate of approximately 0.13 counts per second (cps) at 38 ft. Although very small, the presence of any neutron flux is an indication of transuranic waste.

Historical total gamma data acquired in 1963, 1976, and 1993 indicate a similar profile to that measured by the SGLS in 2006, suggesting no significant contaminant movement.

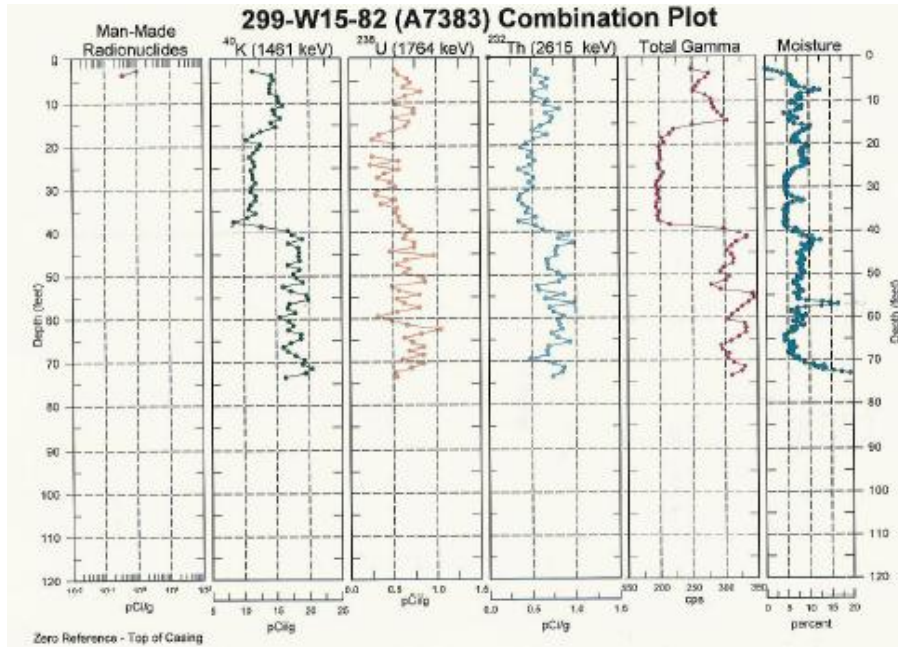


**299-W10-73 (A7163) Manmade Radionuclide Plot**



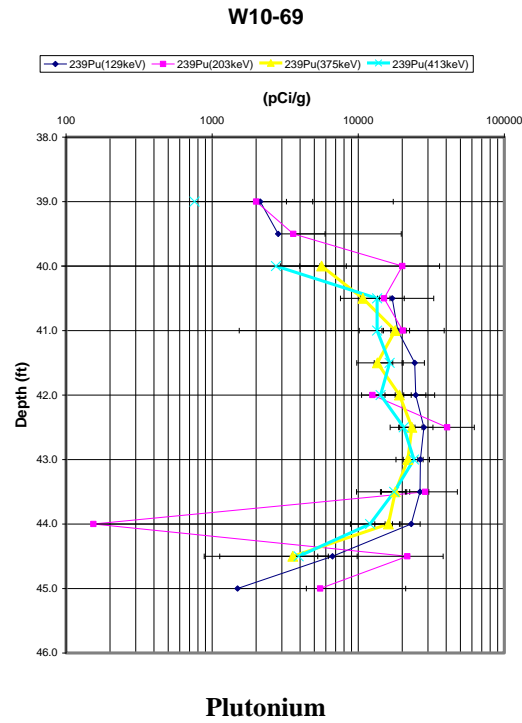
**Well W15-82**

Previous data on well 299-W10-73 (A7163) were obtained from the S. M. Stoller Corp. report HGLP-LDR-036 dated 11/22/06. The report stated that the only manmade radionuclide detected was <sup>137</sup>Cs, which was seen near the ground surface at less than 1 pCi/gram, as shown in the log plots below. No measurements of chlorine or carbon tetrachloride were reported.

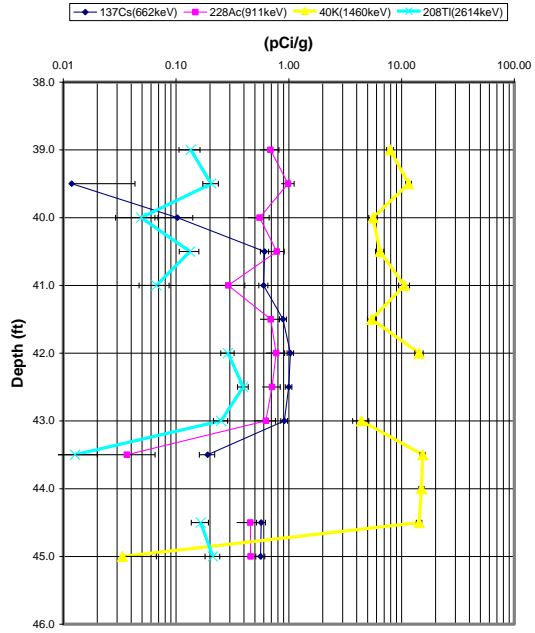


# APPENDIX B: Additional logs obtained at Hanford by APMI

## Additional Passive Gamma Ray logs from Well 10-69



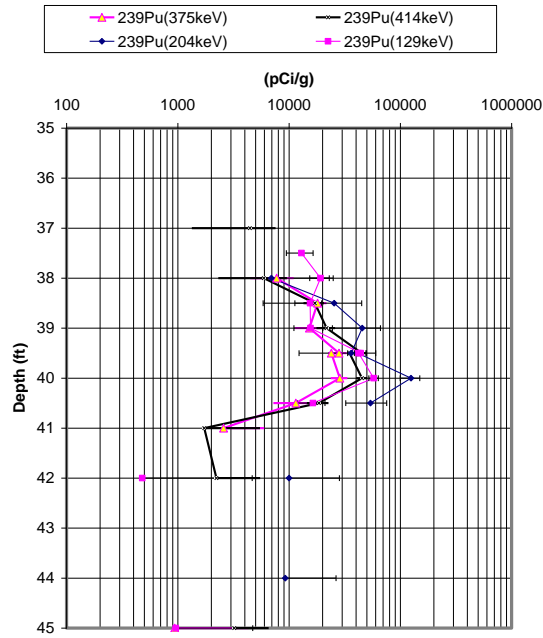
### W10-69



**Cesium, Actinium, Potassium and Thallium**

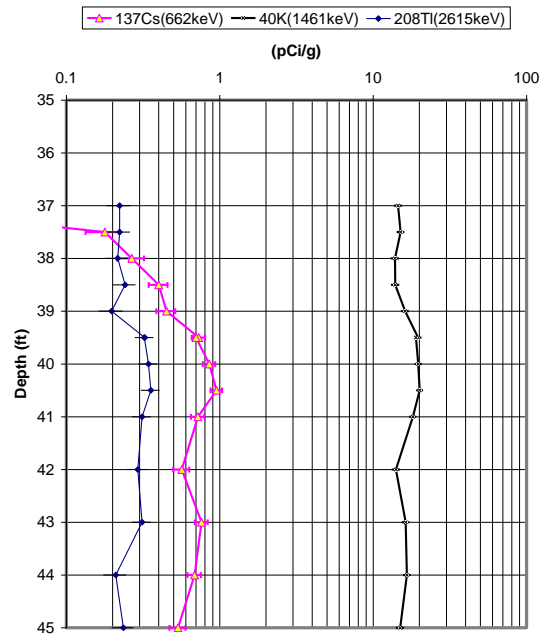
# Additional Passive Gamma Ray logs from Well W10-73

## W10-73



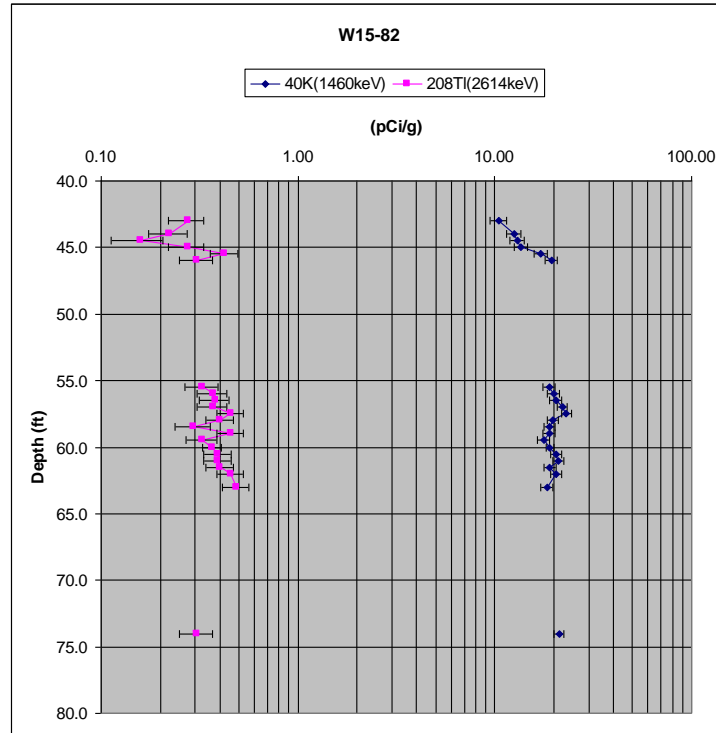
## Plutonium

## W10-73



## Cesium, Potassium and Thallium

## Additional logs from W15-82



$^{40}\text{K}$  and  $^{208}\text{Tl}$  logs for W15-82

### Appendix 3 – Example of MCNP Input and Output Files.

The input file for a typical PNC run is included below. However, the output is so voluminous that it is not included in this report.

First try at a TDT like tool using the zetatron

c Comment summaries included here. For detailed comments see file mgf\_comment

c

1 4 -2.699 -18 19 -15

c

c Cd Wrapping End to Generator Volume (Air)

c r=(5.4625) z=(70.3073,71.27) vol=90.24512cc

c

2 11 -0.00129 -11 14 -13

c

c Generator Al Housing

c r=(4.67,5) z=(71.27,72.27,106.86,107.86) vol=503.84910cc

c

3 4 -2.699 -11 12 -16 17 :-11 16 -2 :-11 -17 13

c

c Air around Generator Al Housing

c r=(5,5.715) z=(71.27,107.86) vol=556.2365cc

c

4 11 -0.00129 11 -1 13 -2

c

c Copper Generator Parts

c r=(.33:1:1:.33) z=(79.2348,83.9848:83.9848,90.36:95.36,99.5:99.5,106.75)

c vol=37.1399cc

c

5 5 -8.94 -5 -4 7 :-5 -8 3 :-6 -7 9 :-6 -10 8

c

c Generator Target 28.5cm to NEAR, 56.34cm to Thermal

c r=(1) z=(90.36,95.36) vol=15.7080cc

c

6 0 -5 4 -3



c

c Fluorinert r=(4.67) z=(72.27,106.86) vol=2317.07491cc

c

7 9 -1.78 -12 17 -16 (5 :4 :-7 )(5 :8 :-3 )(6 :7 :-9 )(6 :10 :-8 )  
(5 :-4 :3 )

c

c \*\*\*\*\*

c

c formation cells using material 27

c

c \*\*\*\*\*

c

- 8 27 -1.605 20 -37 36 -55
- 9 27 -1.605 55 -56 -37 36
- 10 27 -1.605 -56 55 37 -38
- 11 27 -1.605 20 37 -55 -38
- 12 27 -1.605 38 -39 20 -55
- 13 27 -1.605 55 -56 38 -39
- 14 27 -1.605 -56 55 39 -40
- 15 27 -1.605 -55 39 20 -40
- 16 27 -1.605 20 -55 40 -41
- 17 27 -1.605 55 -56 40 -41
- 18 27 -1.605 20 -55 -36 35
- 19 27 -1.605 55 -56 -36 35
- 20 11 -0.00129 -35 20 -55 34
- 21 11 -0.00129 55 -56 -35 34
- 22 22 -1.678 20 -55 -34 33
- 23 22 -1.678 55 -56 -34 33
- 24 22 -1.678 20 -55 -33 32
- 25 22 -1.678 55 -56 -33 32
- 26 22 -1.678 -56 55 -32 31
- 27 22 -1.678 20 -55 -32 31
- 28 22 -1.678 20 -55 -31 30

29 22 -1.678 55 -56 -31 30  
 30 22 -1.678 -30 29 20 -55  
 31 22 -1.678 55 -56 -30 29  
 32 22 -1.678 -29 28 20 -55  
 33 22 -1.678 55 -56 -29 28  
 34 32 -3.67 -64 58 -62 \$Near detector  
 35 32 -3.67 -59 63 -62 \$bottom of far detector  
 37 11 -0.00129 -1 -94 93 61  
 38 11 -0.00129 -1 91 -92  
 39 3 -7.85 36 -37 1 -20  
 40 3 -7.85 -20 1 37 -38  
 41 3 -7.85 -20 1 38 -39  
 42 11 -0.00129 2 -1 -102  
 43 11 -0.00129 102 -103 -1  
 44 11 -0.00129 103 -104 -1  
 45 33 -8.65 -57 64 -61 \$Top cap  
 46 33 -8.65 -61 62 58 -64  
 47 33 -8.65 62 -61 -58 59 \$Cd around PMT's  
 48 33 -8.65 -63 60 -61 \$Bottom Cd piece  
 49 33 -8.65 -61 62 63 -59 \$Side Cd on far detector  
 50 18 -0.66 59 -58 -62

c Spider

51 2 -0.92 -96 78 -68 69 66 -67 (73 :75 :-71 )(70 :76 :73 )  
 (-72 :-74 :70 )(-71 :-72 :-77 )65  
 52 11 -0.00129 -96 -65 61 94  
 53 11 -0.00129 (-1 65 94 -96 (-78 :96 :70 :-76 :73 )(-78 :96 :-70 :71 :-66  
 )(-78 :96 :-71 :-75 :73 )(-78 :96 :-73 :72 :68 )  
 (-78 :96 :-72 :77 :-71 )(71 :-70 :67 :-78 :96 )(70 :74 :-72 :-78 :96  
 )(-73 :72 :-69 :-69 :72 :-73 :-78 :96 )):(70 -71 -1 -66 78 -96 ):  
 (-96 78 73 -72 -1 68 ):(78 -96 -71 70 67 -1 ):(78 -96 73 -72 -69 -1  
 )  
 54 11 -0.00129 89 -90 -1  
 55 11 -0.00129 88 -89 -1

56 11 -0.00129 87 -88 -1  
57 11 -0.00129 86 -87 -1  
58 11 -0.00129 104 -105 -1  
59 11 -0.00129 105 -106 -1  
60 11 -0.00129 106 -107 -1  
61 11 -0.00129 -108 107 -1  
62 11 -0.00129 108 -109 -1  
63 11 -0.00129 109 -110 -1  
64 11 -0.00129 90 -91 -1  
65 22 -1.678 20 -55 -28 27  
66 22 -1.678 55 -56 -28 27  
67 22 -1.678 20 -55 -27 26  
68 22 -1.678 55 -56 -27 26  
69 22 -1.678 20 -26 -55 25  
70 22 -1.678 25 -26 55 -56  
71 22 -1.678 20 -55 -25 24  
72 22 -1.678 55 -56 -25 24  
73 22 -1.678 20 -55 -24 23  
74 22 -1.678 55 -56 -24 23  
75 22 -1.678 20 -23 22 -55  
76 22 -1.678 55 -23 -56 22  
77 27 -1.605 20 41 -55 -42  
78 27 -1.605 55 41 -42 -56  
79 27 -1.605 20 -55 42 -43  
80 27 -1.605 55 -56 42 -43  
81 27 -1.605 20 -55 43 -44  
82 27 -1.605 55 -56 43 -44  
83 27 -1.605 20 44 -55 -45  
84 27 -1.605 44 -45 55 -56  
85 27 -1.605 20 -55 45 -46  
86 27 -1.605 55 -56 45 -46  
87 27 -1.605 20 -55 46 -47  
88 27 -1.605 55 -56 46 -47

89 27 -1.605 56 -47 46 -79  
90 11 -0.00129 79 -80 -47 46  
91 3 -7.85 -81 80 -47 46  
92 25 -2.3 81 -82 -47 46  
93 21 -2.1 82 -83 -47 46  
94 21 -2.1 83 46 -84 -47  
95 21 -2.1 84 -21 -47 46  
96 27 -1.605 56 -46 45 -79  
97 11 -0.00129 79 -80 -46 45  
98 3 -7.85 80 -81 -46 45  
99 25 -2.3 81 -46 -82 45  
100 21 -2.1 82 -83 -46 45  
101 21 -2.1 83 -46 45 -84  
102 21 -2.1 84 -21 -46 45  
103 27 -1.605 56 -79 -45 44  
104 11 -0.00129 79 -80 -45 44  
105 3 -7.85 80 -81 -45 44  
106 25 -2.3 81 -82 -45 44  
107 21 -2.1 82 -45 44 -83  
108 21 -2.1 83 44 -45 -84  
109 21 -2.1 84 -21 -45 44  
110 27 -1.605 56 -44 -79 43  
111 11 -0.00129 79 -80 -44 43  
112 3 -7.85 80 -81 -44 43  
113 25 -2.3 81 -82 -44 43  
114 21 -2.1 82 -44 43 -83  
115 21 -2.1 83 -44 43 -84  
116 21 -2.1 84 -44 -21 43  
117 27 -1.605 56 -43 42 -79  
118 27 -1.605 56 -79 -42 41  
119 27 -1.605 56 -79 -41 40  
120 27 -1.605 56 -79 -40 39  
121 27 -1.605 56 -79 -39 38

122 27 -1.605 56 -79 -38 37  
123 27 -1.605 56 -79 -37 36  
124 27 -1.605 56 -79 -36 35  
125 11 -0.00129 56 -79 -35 34  
126 22 -1.678 56 -79 -34 33  
127 22 -1.678 56 -79 -33 32  
128 22 -1.678 56 -79 -32 31  
129 22 -1.678 56 -79 -31 30  
130 22 -1.678 -79 56 -30 29  
131 22 -1.678 56 -79 -29 28  
132 22 -1.678 56 -79 -28 27  
133 22 -1.678 56 -79 -27 26  
134 22 -1.678 56 -79 -26 25  
135 22 -1.678 56 -79 -25 24  
136 22 -1.678 56 -79 -24 23  
137 22 -1.678 -79 56 -23 22  
138 11 -0.00129 79 -80 -43 42  
139 11 -0.00129 -80 79 -42 41  
140 11 -0.00129 79 -80 -41 40  
141 11 -0.00129 79 -80 -40 39  
142 11 -0.00129 79 -80 -39 38  
143 11 -0.00129 79 -80 -38 37  
144 11 -0.00129 79 -80 -37 36  
145 11 -0.00129 79 -80 35 -36  
146 11 -0.00129 79 -80 -35 34  
147 11 -0.00129 -34 33 79 -80  
148 11 -0.00129 79 -80 -33 32  
149 11 -0.00129 79 -80 -32 31  
150 11 -0.00129 79 -80 -31 30  
151 11 -0.00129 -80 79 -30 29  
152 11 -0.00129 79 -80 28 -29  
153 11 -0.00129 79 -80 -28 27  
154 11 -0.00129 79 79 -80 -27 26

155 11 -0.00129 -80 79 -26 25  
156 11 -0.00129 79 -80 -25 24  
157 11 -0.00129 79 -80 -24 23  
158 11 -0.00129 -80 79 -23 22  
159 3 -7.85 -81 80 42 -43  
160 3 -7.85 -81 80 -42 41  
161 3 -7.85 -81 80 -41 40  
162 3 -7.85 80 -81 -40 39  
163 3 -7.85 80 -81 -39 38  
164 3 -7.85 80 -81 -38 37  
165 3 -7.85 80 -81 -37 36  
166 3 -7.85 -81 80 -36 35  
167 3 -7.85 80 -81 -35 34  
168 3 -7.85 80 -81 -34 33  
169 3 -7.85 -81 80 -33 32  
170 3 -7.85 80 -81 -32 31  
171 3 -7.85 80 -81 -31 30  
172 3 -7.85 80 -81 -30 29  
173 3 -7.85 80 -81 -29 28  
174 3 -7.85 80 -81 -28 27  
175 3 -7.85 80 -81 -27 26  
176 3 -7.85 80 -81 -26 25  
177 3 -7.85 80 -81 -25 24  
178 3 -7.85 80 -81 -24 23  
179 3 -7.85 -81 80 -23 22  
180 25 -2.3 81 -43 42 -82  
181 25 -2.3 81 -82 -42 41  
182 25 -2.3 81 -82 -41 40  
183 25 -2.3 81 -82 -40 39  
184 25 -2.3 81 -82 -39 38  
185 25 -2.3 81 -82 -38 37  
186 25 -2.3 81 -82 -37 36  
187 25 -2.3 81 -82 -36 35

188 25 -2.3 81 -82 -35 34  
189 25 -2.3 81 -82 -34 33  
190 25 -2.3 81 -82 -33 32  
191 25 -2.3 81 -82 -32 31  
192 25 -2.3 81 -82 -31 30  
193 25 -2.3 -82 81 -30 29  
194 25 -2.3 81 -82 -29 28  
195 25 -2.3 81 -82 -28 27  
196 25 -2.3 81 -82 -27 26  
197 25 -2.3 81 -82 -26 25  
198 25 -2.3 81 -82 -25 24  
199 25 -2.3 81 -82 -24 23  
200 25 -2.3 -82 81 22 -23  
201 21 -2.1 82 -43 -83 42  
202 21 -2.1 83 -43 42 -84  
203 21 -2.1 84 -43 -21 42  
204 21 -2.1 82 -42 -83 41  
205 21 -2.1 41 -42 83 -84  
206 21 -2.1 41 84 -42 -21  
207 21 -2.1 82 -41 -83 40  
208 21 -2.1 83 -41 -84 40  
209 21 -2.1 84 -41 -21 40  
210 21 -2.1 82 -40 39 -83  
211 21 -2.1 83 -40 -84 39  
212 21 -2.1 84 -40 -21 39  
213 21 -2.1 82 -39 -83 38  
214 21 -2.1 83 -39 -84 38  
215 21 -2.1 38 84 -39 -21  
216 21 -2.1 82 -38 -83 37  
217 21 -2.1 83 -38 -84 37  
218 21 -2.1 84 -38 -21 37  
219 21 -2.1 82 -37 -83 36  
220 21 -2.1 83 -37 -84 36

221 21 -2.1 36 84 -37 -21  
222 21 -2.1 82 -36 -83 35  
223 21 -2.1 83 -36 -84 35  
224 21 -2.1 84 -36 -21 35  
225 21 -2.1 82 -35 -83 34  
226 21 -2.1 83 -35 -84 34  
227 21 -2.1 84 -35 -21 34  
228 21 -2.1 82 -34 -83 33  
229 21 -2.1 83 -34 -84 33  
230 21 -2.1 84 -34 -21 33  
231 21 -2.1 82 -33 -83 32  
232 21 -2.1 83 -33 32 -84  
233 21 -2.1 84 -33 -21 32  
234 21 -2.1 82 -32 -83 31  
235 21 -2.1 83 -32 -84 31  
236 21 -2.1 84 -32 -21 31  
237 21 -2.1 82 -31 -83 30  
238 21 -2.1 83 -31 -84 30  
239 21 -2.1 84 -31 -21 30  
240 21 -2.1 82 -30 -83 29  
241 21 -2.1 83 -30 -84 29  
242 21 -2.1 84 -30 -21 29  
243 21 -2.1 82 -29 -83 28  
244 21 -2.1 83 -29 -84 28  
245 21 -2.1 84 -29 -21 28  
246 21 -2.1 82 -28 -83 27  
247 21 -2.1 83 -28 -84 27  
248 21 -2.1 84 -28 -21 27  
249 21 -2.1 82 -27 -83 26  
250 21 -2.1 83 -27 -84 26  
251 21 -2.1 84 -21 -27 26  
252 21 -2.1 82 -26 -83 25  
253 21 -2.1 83 -26 -84 25



254 21 -2.1 84 -26 -21 25  
255 21 -2.1 82 -25 -83 24  
256 21 -2.1 83 -25 24 -84  
257 21 -2.1 84 -25 -21 24  
258 21 -2.1 82 -24 -83 23  
259 21 -2.1 83 -24 -84 23  
260 21 -2.1 84 -24 -21 23  
261 21 -2.1 82 -23 -83 22  
262 21 -2.1 83 -23 22 -84  
263 21 -2.1 84 -23 -21 22  
264 11 -0.00129 -35 -20 1 34  
265 3 -7.85 -34 -20 33 1  
266 11 -0.00129 11 -1 -13 96  
267 11 -0.00129 -14 15 -18  
268 4 -2.699 -61 57 -19  
269 11 -0.00129 (96 -14 -11 18 );(96 -19 -18 61 )  
270 3 -7.85 32 1 -20 -33  
271 3 -7.85 -20 1 31 -32  
272 3 -7.85 -20 1 39 -40  
273 3 -7.85 -20 1 40 -41  
274 3 -7.85 -20 1 -42 41  
275 3 -7.85 -20 1 42 -43  
276 3 -7.85 -20 1 43 -44  
277 3 -7.85 -20 1 44 -45  
278 3 -7.85 -20 1 45 -46  
279 3 -7.85 -20 1 -47 46  
280 3 -7.85 -20 1 -31 30  
281 3 -7.85 -20 1 -30 29  
282 3 -7.85 -20 1 -29 28  
283 3 -7.85 -20 1 -28 27  
284 3 -7.85 -20 1 -27 26  
285 3 -7.85 -20 1 -26 25  
286 3 -7.85 -20 1 -25 24

287 3 -7.85 -20 1 -24 23  
288 3 -7.85 -20 1 -23 22  
289 11 -0.00129 -1 -86 85  
290 3 -7.85 -20 1 -36 35  
291 21 -2.1 -21 84 47 -48  
292 21 -2.1 -84 47 -48 83  
293 21 -2.1 -83 47 82 -48  
294 25 -2.3 -82 81 47 -48  
295 3 -7.85 -81 80 47 -48  
296 11 -0.00129 -80 79 47 -48  
297 27 -1.605 -79 47 56 -48  
298 27 -1.605 -56 47 55 -48  
299 27 -1.605 -55 20 -48 47  
300 3 -7.85 -20 1 -48 47  
301 21 -2.1 48 84 -21 -49  
302 21 -2.1 -84 48 83 -49  
303 21 -2.1 -83 48 82 -49  
304 25 -2.3 -82 48 81 -49  
305 3 -7.85 -81 80 48 -49  
306 25 -2.3 -80 48 -49 79  
307 27 -1.605 -79 48 56 -49  
308 27 -1.605 -56 48 55 -49  
309 27 -1.605 -55 20 48 -49  
310 3 -7.85 1 -20 -49 48  
311 21 -2.1 -21 -50 84 49  
312 21 -2.1 -84 83 49 -50  
313 21 -2.1 -83 82 49 -50  
314 25 -2.3 -82 81 49 -50  
315 3 -7.85 -81 80 -50 49  
316 11 -0.00129 -80 79 49 -50  
317 27 -1.605 -79 49 -50 56  
318 27 -1.605 -56 49 55 -50  
319 27 -1.605 -55 49 20 -50

320 3 -7.85 -20 1 -50 49  
 321 11 -0.00129 110 -111 -1  
 322 11 -0.00129 -1 111 -112  
 323 11 -0.00129 112 -113 -1  
 324 2 -0.92 -114 -116 117 (61 :-60 )(114 :-115 :-117 :60 )  
 325 11 -0.00129 (-93 92 -1 61 (114 :116 :-60 :-61 )(115 :-117 :60 :-61 )):  
 (-61 -117 92 )  
 326 21 -2.1 -22 51 -21 84  
 327 21 -2.1 -84 -22 83 51  
 328 21 -2.1 -83 -22 82 51  
 329 25 -2.3 -82 -22 51 81  
 330 3 -7.85 -81 80 -22 51  
 331 11 -0.00129 -80 79 51 -22  
 332 22 -1.678 -79 56 51 -22  
 333 22 -1.678 -56 -22 55 51  
 334 22 -1.678 -55 -22 20 51  
 335 3 -7.85 -20 1 51 -22  
 336 21 -2.1 -51 -21 84 52  
 337 21 -2.1 -84 -51 83 52  
 338 21 -2.1 -83 82 -51 52  
 339 25 -2.3 -82 81 -51 52  
 340 3 -7.85 -81 80 -51 52  
 341 11 -0.00129 -80 79 -51 52  
 342 22 -1.678 -79 -51 56 52  
 343 22 -1.678 -56 -51 52 55  
 344 22 -1.678 -55 20 -51 52  
 345 3 -7.85 1 -20 -51 52  
 346 11 -0.00129 -1 -85 54  
 347 11 -0.00129 -1 -54 53  
 348 0 ((21 :50 :-52 )(1 :113 )):(-53 -1 ):(113 -1 )

1 cz 5.715 \$Inner wall of Penetrometer

2 pz 107.86

3 pz 95.36  
4 pz 90.36  
5 cz 1  
6 cz 0.33  
7 pz 83.9848  
8 pz 99.5  
9 pz 79.2348  
10 pz 106.75  
11 cz 5  
12 cz 4.67  
13 pz 71.27  
14 pz 70.3073 \$ Generator end of Cd wrap  
15 pz 70.1752 \$ Inside of Cd wrap on Generator end  
16 pz 106.86  
17 pz 72.27  
18 cz 3.01625  
19 pz 62.5552 \$ Generator end of Top Al Spacer  
20 cz 6.985 \$ Penetrometer pipe outer wall  
21 cz 80 \$outer boundary  
22 1 pz -60 \$bottom of system  
23 1 pz -50  
24 1 pz -40  
25 1 pz -30  
26 1 pz -20  
27 1 pz -10  
28 1 pz 0  
29 1 pz 10  
30 1 pz 20  
31 1 pz 30  
32 1 pz 40  
33 1 pz 50  
34 1 pz 60  
35 1 pz 70

36 1 pz 80  
37 1 pz 90  
38 1 pz 100  
39 1 pz 110  
40 1 pz 120  
41 1 pz 130  
42 1 pz 140  
43 1 pz 150  
44 1 pz 160  
45 1 pz 170  
46 1 pz 180  
47 1 pz 190  
48 1 pz 200  
49 1 pz 210  
50 1 pz 220  
51 1 pz -70  
52 1 pz -80  
53 pz -80  
54 pz -70  
55 cz 15  
56 cz 25  
57 pz 62.076 \$outside of top detector Cadmium  
58 pz 54.5 \$Bottom of near detector  
59 pz 31.5 \$top of far detector  
60 pz 16.424 \$bottom of Far detector  
61 cz 1.346  
62 cz 1.27

c bottom Cadmium (30 mils)

63 pz 16.5  
64 pz 62 \$inside of near Cd shield  
65 cz 1.6002  
66 px -4.826  
67 px 4.826

68 py 4.826  
69 py -4.826  
70 py -0.635  
71 py 0.635  
72 px 0.635  
73 px -0.635  
74 p 1 -1 0 2.921  
75 p 1 -1 0 -2.921  
76 p 1 1 0 -2.921  
77 p 1 1 0 2.921  
78 pz 38.57  
79 cz 34.29 \$outside of drum  
80 cz 37 \$inside of steel caisson  
81 cz 38.27 \$O.D. of caisson  
82 cz 42.08 \$O.D. of cement annulus  
83 cz 52.08  
84 cz 66  
85 pz -60  
86 pz -50  
87 pz -40  
88 pz -30  
89 pz -20  
90 pz -10  
91 pz 0  
92 pz 10  
93 pz 20  
94 pz 30  
95 pz 40  
96 pz 50  
97 pz 60  
98 pz 70  
99 pz 80  
100 pz 90

101 pz 100  
102 pz 110  
103 pz 120  
104 pz 130  
105 pz 140  
106 pz 150  
107 pz 160  
108 pz 170  
109 pz 180  
110 pz 190  
111 pz 200  
112 pz 210  
113 pz 220  
114 cz 3.4925  
115 cz 2.8575  
116 pz 17.059 \$Top of plastic disk  
117 pz 15.789 \$bottom of plastic disc

tr1 0 0 0

mode n p

c cut:N 3.0E6 0.0 -0.5 -0.25

c sdef cel=900 erg=d1 pos= 0 5.6 30.48

c sp1 -3 1.136 2.0

c

c ++++++

c

c DATA

c

c ++++++

c

c MATERIALS and densities (g/cc)

c 1 Helium-3 0.001071,0.000714 (4,6 atm)

c 2 Virgin Poly 0.92\*

c	3 Carbon Steel	7.81				
c	4 Aluminum	2.699				
c	5 Copper	8.94				
c	6 Boroflex					
c	7 304 SSTL	8.027				
c	8 Cadmium	8.65				
c	9 Flourinert	1.78				
c	10 Wet Water	1.0				
c	11 Air	0.00129				
c	12 WG Plutonium	19.6				
c	21 Surrogate 1 Mix	1.6258				
c	22 Surrogate 3 Mix	1.6046				
c	23 Surrogate 3 Mix	1.6820				
c	24 Surrogate 4 Mix	1.6270				
c	25 Concrete	2.3				
c	26 Surrogate #3 mix					
c	27 Surrogate 5 Mix	1.6958				
c						
m1	2003.	-1 \$MAT				
m2	1001.	-0.1437 \$MAT				
	6000.	-0.8563				
m3	6000.	-0.009935 \$MAT				
	26054.	-0.05546	26056.	-0.9095	26057.	-0.0222
	26058.	-0.002905				
m4	13027.	-1 \$MAT				
m5	29063.	-0.685 \$MAT				
	29065.	-0.315				
c	m6	1001 -0.0276	5010 -0.05	5011 -0.203		
c	6000	-0.2019	8016 -0.2426	14000 -0.270393194		
c	20000	-0.0004				
c	26054	-2.297e-4	26056	-3.766e-3	26057	-9.196e-5
c	26058	-1.191e-5				
m7	6000.	-0.0008 \$MAT				



14000. -0.01 15031. -0.00045 16000. -0.0003  
24050. -0.007939 24052. -0.159 24053. -0.01838  
24054. -0.004652 25055. -0.02 26054. -0.03801  
26056. -0.623282 26057. -0.01522 26058. -0.001971  
28058. -0.0672 28060. -0.02677 28061. -0.001183  
28062. -0.00383 28064. -0.001013

m8 48000. -1 \$MAT

c

c Material #9 is Polyurethane Resin

c

c m9 1001 -3.9596 -2 6000 -2.0222 -1

c 7014 -7.8605 -2 8016 -1.7958 -1

c

m9 6000. -0.231 \$MAT

8016. -0.038 9019. -0.731

m10 1001. -0.1119 \$Water

8016. -0.8881

m11 7014. -0.755 \$MAT

8016. -0.232 18000. -0.013

m12 94238. 0.00015 \$Pu

94239. 0.9395 94240. 0.0587 94241. 0.0014

94242. 0.00025

c

c =====

c ===== Material # 18

c =====

c Name = PMT mix

c Density = 0.6550 g/cc

c

m18 8016. 0.436352 \$MAT

14000. 0.218176 26000. 0.345473

c

m21 1001. -0.00326 \$MAT

7014.	-0.001411	8016.	-0.539776	13027.	-0.029093
14000.	-0.426437	18000.	-2.4e-005		
m22 1001.	-0.00347 \$Sand 27 Sur #3				
7014.	-0.00119	8016.	-0.29743	13027.	-0.01468
14000.	-0.23813	18000.	-2e-005	6000.	-0.02176
11023.	-0.16699	17000.	-0.25753		
m23 1001.	-0.00503 \$MAT				
7014.	-0.001153	8016.	-0.297782	13027.	-0.014665
14000.	-0.237309	18000.	-2.5e-005	6000.	-0.020162
11023.	-0.171073	17000.	-0.252807		
m24 1001.	-0.01683 \$MAT				
7014.	-0.001587	8016.	-0.568341	13027.	-0.150187
14000.	-0.263028	18000.	-2.7e-005		
m25 1001.	-0.0179 \$Cement				
7014.	-0.045	8016.	-0.5518	12000.	-0.0013
13027.	-0.0048	14000.	-0.3245	18000.	-0.0008
20000.	-0.0487	26056.	-0.0049		
m26 8016.	-0.5326 \$MAT				
14000.	-0.4674				
m27 1001.	-0.01687 \$Sand 27 Sur #4				
7014.	-0.00119	8016.	-0.56857	13027.	-0.15048
14000.	-0.26409	18000.	-2e-005		
m31 1001.	-0.004671 \$Sludge				
8016.	-0.48955	12000.	-0.002336	13027.	-0.007007
14000.	-0.239583	16000.	-0.025218	17000.	-0.029184
6000.	-0.116756	20000.	-0.052771	26000.	-0.03196
94239.	-0.000965				
m32 53129.60c	0.5 \$NaI				
11023.62c	0.5				
m33 48000.51c	1 \$Cadmium				
c					
c	uniform importances				
c					

imp:n 1 345r 0 \$ 1, 348

imp:p 1 345r 0 \$ 1, 348

c

c made from tdtgap2 and wwfromtdtgap2o

c

c

c The source below is a Cf-252 source following a

c Watt fission energy spectrum

c  $p(E) = C \exp(-E/a) \sinh(\sqrt{bE})$

c with  $a=1.136$   $b=2.0$

c

c

nps 30000000

c

c

c \*\*\*\*\*

c

c SOURCE CARD

c

c \*\*\*\*\*

c

c Note : Do not start particle on a cell boundary, it will get lost!!!!

c

c The source below in a 14 MeV neutron generator originating in the

c target cell distributed in time according to the distribution sp1 vs si1.

c The distribution is from 0 to 100 usec (0 to 10000 shakes) and is

c roughly 10-15 usec wide

c

c ctme 225

c changes -dcm

c wwge:n 0.414e-6 1.e-4 1.e-2 1 14.2

wwg 14 6 .9 4j 1

wwge:n 3000 7500 20000 60000

wwge:p 3000 7500 20000 60000

c

cut:n 1.5e5 0.0 -0.5 -0.25

sdef tme=d1 pos= 0 0 92.5

si1 0 100 200 300 400 500 600 700 800 900

1000 1100 1200 1300 1400 1500 1600 1700 1800 1900

2000 2100 2200 2300 2400 2500 2600 2700 2800 2900

sp1 0 5.4801E-4 5.6993078E-2 1.23959945E-1 8.2859167E-2

8.1763147e-2 8.044792E-2 0.089435292 0.101929928 0.097765049

0.084722403 0.065651642 0.046690483 0.032990224 0.018741955

0.009316176 0.005370502 0.004164879 0.002959256 0.00263045

0.002055039 0.001430307 0.001019299 0.000739814 0.000558971

0.000435668 0.000361687 0.000316476 0.000287705 0.000267155

mt2 poly.01t

c

f4:p 34

fq4 e t m

f14:p 35

fq14 e t m

c

c Default time bins for neutron generator runs

c

c Default time bins for Cf-252 runs

c

c t0 0 150000

c

t4 500 1000 1500 2000 2500 3000 3500 4000 4500 5000

5500 6000 7000 8000 9000 12000 15000 18000 21000 24000

27000 30000 33000 36000 39000 42000 45000 48000 51000 54000

57000 60000 63000 66000 69000 72000 75000 78000 81000 84000

87000 90000 93000 96000 99000

t14 500 1000 1500 2000 2500 3000 3500 4000 4500 5000

5500 6000 7000 8000 9000 12000 15000 18000 21000 24000

27000 30000 33000 36000 39000 42000 45000 48000 51000 54000  
57000 60000 63000 66000 69000 72000 75000 78000 81000 84000  
87000 90000 93000 96000 99000

print

AN EXAMPLE OF THE OUTPUT FROM A MCNP RUN WITH THE ABOVE AS INPUT: